JOC Article
pubs.acs.org/joc

Synthesis and Photophysical Properties of N-Fused Tetraphenylporphyrin Derivatives: Near-Infrared Organic Dye of [18]Annulenic Compounds

Shinya Ikeda,[†] Motoki Toganoh,[†] Shanmugam Easwaramoorthi,[‡] Jong Min Lim,[‡] Dongho Kim,*[,‡] and Hiroyuki Furuta*[,†]

[†]*Department of Chemistry and Biochemistry, Graduate School of Engineering, Kyushu University, 744 Moto-oka, Nishi-ku, Fukuoka 819-0395, Japan, and* [‡]*Spectroscopy Laboratory for Functional π-electronic Systems and Department of Chemistry, Yonsei University, Seoul 120-749, Korea*

hfuruta@cstf.kyushu-u.ac.jp; dongho@yonsei.ac.kr

Received October 28, 2010

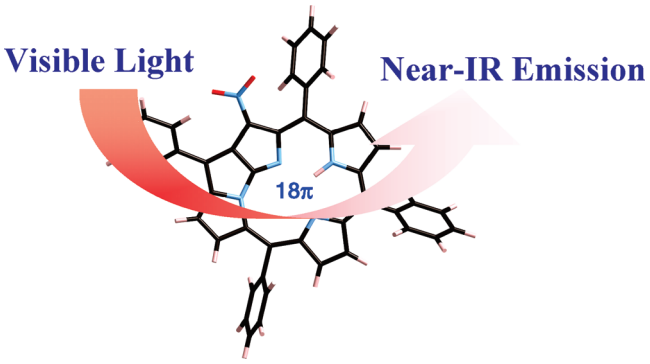

A variety of N-fused porphyrin derivatives were prepared and their photophysical properties were investigated. Although intact N-fused tetraarylporphyrins showed almost no emission, introduction of electron-withdrawing groups such as a nitro group and a cyano group on the macrocycles caused significant refinements in their emission efficiency. Long emission wavelengths (900−1000 nm) as well as fairly large Stokes shifts (~1200 cm^{-1}) are exceptionally unique photophysical properties among [18]annulenic compounds, which could be rationalized by the excited state intramolecular proton transfer (ESIPT) process. Relatively weak emission quantum yields (~5.0×10^{-4}) and unusually short S_1 state lifetimes (~13.5 ps) are in good agreement with the ESIPT process. The solvent and substituent effects on the photophysical properties are also discussed in conjunction with the theoretical studies, where the mesityl groups at the *meso*-positions play a unique role.

Introduction

Development of near-infrared (NIR) emissive organic materials is highly expected because of their promising applications in biosensing probes, optical communication, photovoltaics, and solar cells.[1] These organic materials commonly require extensively large π-conjugated systems to achieve a narrow HOMO−LUMO band gap. Resultingly, they typically have elaborate structures and often suffer from tedious synthetic procedures and chemical/physical instability. Nevertheless, the outstanding achievement in the field of NIR emissive organic materials has been obtained with cyanine dyes and π-extended porphyrins.[2,3]

(1) (a) Fibian, J.; Nakazumi, H.; Matsuoka, M. *Chem. Rev.* **1992**, *92*, 1197. (b) Weissleder, R.; Ntziachristos, V. *Nat. Med.* **2003**, *9*, 123. (c) Roncali, J. *Chem. Rev.* **1997**, *97*, 173. (d) Kertesz, M.; Choi, C. H.; Yang, S. *Chem. Rev.* **2005**, *105*, 3448. (e) Frangioni, J. V. *Curr. Opin. Chem. Biol.* **2003**, *7*, 626. (f) Weissleder, R. *Nat. Biotechnol.* **2001**, *19*, 316. (g) Hagfeldt, A.; Grätzel, M. *Acc. Chem. Res.* **2000**, *33*, 269. (h) Imahori, H.; Uneyama, T.; Ito, S. *Acc. Chem. Res.* **2009**, *42*, 1809. (i) Mishra, A.; Fischer, M. K. R.; Bäuerle, P. *Angew. Chem., Int. Ed.* **2009**, *48*, 2474.

(2) (a) Kiyose, K.; Kojima, H.; Urano, Y.; Nagano, T. *J. Am. Chem. Soc.* **2006**, *128*, 6548. (b) Perlitz, C.; Licha, K.; Scholle, F.-D.; Ebert, B.; Bahner, M.; Hauff, P.; Moesta, K. T.; Schirner, M. *J. Fluoresc.* **2005**, *15*, 443.

(3) (a) Sessler, J. L.; Seidel, D. *Angew. Chem., Int. Ed.* **2003**, *42*, 5134. (b) Duncan, T. V.; Susumu, K.; Sinks, L. E.; Therien, M. J. *J. Am. Chem. Soc.* **2006**, *128*, 9000. (c) Ryu, J.-H.; Nagamura, T.; Nagai, Y.; Matsumoto, R.; Furuta, H.; Nakamura, K. *Mol. Cryst. Liq. Cryst.* **2006**, *445*, 249. (d) Kwon, J. H.; Ahn, T. K.; Yoon, M.-C.; Kim, D. Y.; Koh, M. K.; Kim, D.; Furuta, H.; Suzuki, M.; Osuka, A. *J. Phys. Chem. B* **2006**, *110*, 11683. (e) Xie, Y.-S.; Yamaguchi, K.; Toganoh, M.; Uno, H.; Suzuki, M.; Mori, S.; Saito, S.; Osuka, A.; Furuta, H. *Angew. Chem., Int. Ed.* **2009**, *48*, 5496.

DOI: 10.1021/jo102128m Published on Web 11/17/2010

CHART 1. Ring-Fused Porphyrinoids

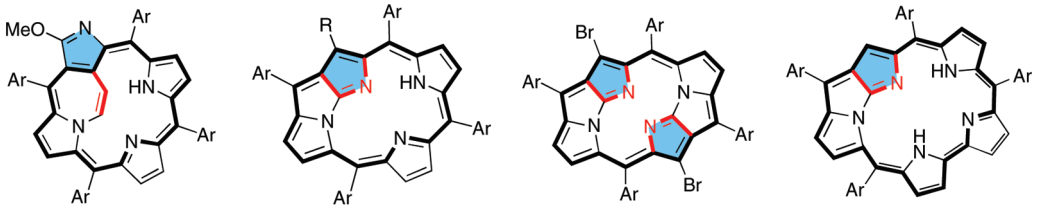

etheno-bridged N-confused porphyrin | N-fused porphyrin | doubly N-fused porphyrin | N-fused sapphyrin

We have recently developed a unique strategy, "ring-fusion", to achieve a narrow HOMO−LUMO band gap with the relatively small-sized molecules (Chart 1).[4−7] Thus, fusion of two adjacent pyrrole rings in the porphyrinoid skeletons caused a remarkable decrease of the HOMO−LUMO band gap without increasing the number of π-electrons. For example, the absorption edges of N-fused porphyrin (NFP) and doubly N-fused porphyrin (N_2FP) exceeded 1000 and 1600 nm, respectively.[5,6] These wavelengths are exceptionally large among [18]annulenic compounds. Similarly, etheno-bridged N-confused porphyrins also showed the significant red-shifts in the absorption spectra.[7] Although these compounds would be favorable for NIR emissive materials, their emission properties have not yet been studied. This time, a variety of N-fused tetraphenylporphyrin (NFTPP) derivatives were prepared and their photophysical properties were investigated to reveal that the NFTPP derivatives showed definite fluorescence in the NIR region with large Stokes shifts. This is a peculiar example of small-sized NIR emissive organic compounds.

Results and Discussion

Preparation of NFTPP Derivatives. Preparation of NFTPP derivatives basically followed the reported procedures (Scheme 1).[5] Nitration of N-confused porphyrin (NCP, **7**)[8] with $NaNO_2$/HCl gave 21-NO_2-NCP (**8**)[9] in 62−74% yields and subsequent bromination with *N*-bromosuccinimide (NBS) gave 3-Br-21-NO_2-NCP (**9**) in 61−79% yields. Treatment of **9** with pyridine afforded 21-NO_2-NFP (**1**) in 60−82% yields. Alternatively, the reactions of **7** with 2 equiv of NBS afforded 3,21-Br_2-NCP (**10**) and subsequent treatment with pyridine gave 21-Br-NFP (**3**) in 35−69% yields (2 steps). Debromination of **3** gave the intact NFP (**2**) in 44−63% yields and Pd-catalyzed coupling reactions of **3a** gave 21-CN-NFP (**4a**) and 21-alkynyl-NFP (**5a**) in 45% and 16% yields, respectively.[10] In the synthesis of a series of 21-NO_2-NFPs (**1**) from NCP (**7**), no obvious trend between the product yields and the electronic as well as the steric effect of *meso*-aryl groups was observed. All the reactions proceeded in moderate to good yields (60−82% yields). Meanwhile, in the cases of 4-trifluoromethylphenyl and mesityl derivatives, formation of **1** from **9** was very slow and not efficient. Hence **1f** and **1g** were prepared from **3f** (44% yield) and **3g** (84% yield), respectively, by a treatment with $AgNO_2$. 21-Cl-NFP (**6a**) was also prepared from **7a** (55% yield in 3 steps) in a similar manner as **1a**.

Absorption Spectroscopy. The absorption spectra of selected NFTPP derivatives in CH_2Cl_2 are shown in Figure 1 together with the calculated oscillator strengths at the B3LYP/6-311++G**//B3LYP/6-31G** level. Numerical data are summarized in Table 1. Compared to the parent compound, NFTPP (**2a**, entry 1), significant blue-shifts in the Q-like bands are observed by introducing a nitro group at the 21-position (**1a**, entry 3). Besides, the discernible difference between the UV−vis−NIR absorption spectrum of **1a** and that of **2a** was found in the vibratory fine structures (Figure 1a,b). The first and second Q-like absorption bands in **2a** are clearly split in two, possibly due to the vibration levels. The time-dependent density functional theory (TD-DFT) calculations on **2a** supported this hypothesis, in which only two transitions were obtained in the region from 600 to 1000 nm. In contrast, splitting of the Q-like bands became ambiguous in the UV−vis−NIR absorption spectra of **1a**. Introduction of a set of functional groups into the *meso*-aryl moieties of **1a** resulted in a fine-tuning of the electronic states. While the electron-donating groups led to the red-shifts (entries 4−7), the electron-withdrawing groups induced the slight blue-shifts (entry 8) in the absorption spectra. In spite of the electron-donating nature of the methyl groups, a significant blue-shift from **1a** is observed in **1g** (entry 9). A similar blue-shift is also seen in **2g** compared to **2a** (entry 2). This unique trend imposed by the mesityl groups is probably due to the steric repulsion aroused by the *o*-methyl groups and it is discussed below in detail. Introduction of the halogen atoms at the 21-position caused small red-shifts (entries 10−11) and introduction of an alkynyl group caused a large red-shift (entry 12). In the case of 21-CN-NFTPP (**4a**, entry 13), a significant blue-shift is observed in a similar manner to 21-NO_2-NFPs. The molar absorption coefficients of NFTPP derivatives are not so different from that of the parent compound **2a**.

Substituent Effect. The electronic perturbation caused by the nitro group at the 21-position of the NFTPP was

(4) (a) Gupta, I.; Srinivasan, A.; Morimoto, T.; Toganoh, M.; Furuta, H. *Angew. Chem., Int. Ed.* **2008**, *47*, 4563. (b) Park, J. K.; Yoon, Z. S.; Yoon, M.-C.; Kim, K. S.; Mori, S.; Shin, J.-Y.; Osuka, A.; Kim, D. *J. Am. Chem. Soc.* **2008**, *130*, 1824. (c) Srinivasan, A.; Ishizuka, T.; Maeda, H.; Furuta, H. *Angew. Chem., Int. Ed.* **2004**, *43*, 2951.

(5) (a) Furuta, H.; Ishizuka, T.; Osuka, A.; Ogawa, T. *J. Am. Chem. Soc.* **1999**, *121*, 2945. (b) Furuta, H.; Ishizuka, T.; Osuka, A.; Ogawa, T. *J. Am. Chem. Soc.* **2000**, *122*, 5748.

(6) Toganoh, M.; Kimura, T.; Uno, H.; Furuta, H. *Angew. Chem., Int. Ed.* **2008**, *47*, 8913.

(7) (a) Toganoh, M.; Kimura, T.; Furuta, H. *Chem. Commun.* **2008**, 102. (b) Toganoh, M.; Kimura, T.; Furuta, H. *Chem.—Eur. J.* **2008**, *14*, 10585. (c) Toganoh, M.; Hihara, Y.; Furuta, H. *Inorg. Chem.* **2010**, *49*, 8182.

(8) (a) Furuta, H.; Asano, T.; Ogawa, T. *J. Am. Chem. Soc.* **1994**, *116*, 767. (b) Chmielewski, P. J.; Latos-Grażyński, L.; Rachlewicz, K.; Głowiak, T. *Angew. Chem., Int. Ed. Engl.* **1994**, *33*, 779.

(9) (a) Ishikawa, Y.; Yoshida, I.; Akaiwa, K.; Koguchi, E.; Sasaki, T.; Furuta, H. *Chem. Lett.* **1997**, *26*, 453. (b) Hung, C. H.; Liaw, C. C.; Chin, W. M.; Chang, G. F.; Chuang, C. H. *J. Porphyrins Phthalocyanines* **2006**, *10*, 953.

(10) Ishizuka, T.; Ikeda, S.; Toganoh, M.; Yoshida, I.; Ishikawa, Y.; Osuka, A.; Furuta, H. *Tetrahedron* **2008**, *64*, 4037.

SCHEME 1. Preparation of NFTPP Derivatives

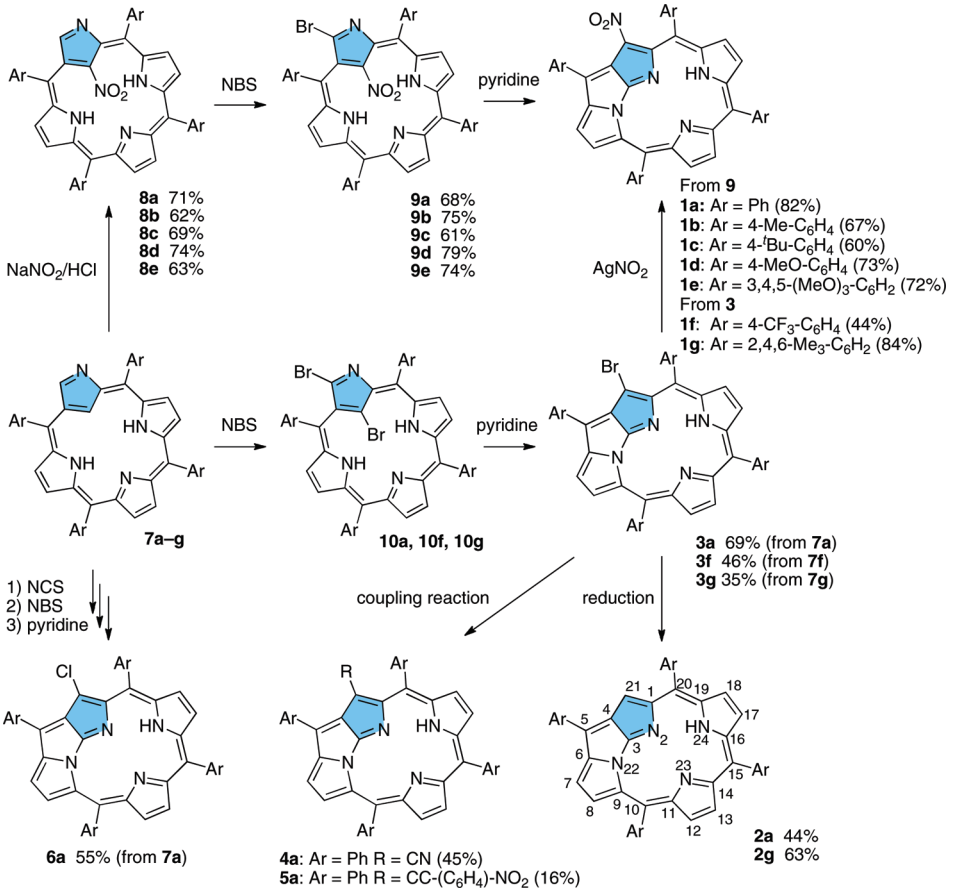

analyzed with the aid of DFT calculations. The Kohn−Sham orbitals of **1a** and **2a** calculated at the B3LYP/6-31G** level are shown in Figure 2a−d. Apparently, the LUMO of **1a** and that of **2a** closely resemble each other. No contribution of the nitro group is observed. In contrast, the nitro group contributes significantly to the HOMO of **1a**. Accordingly, the HOMO would be stabilized strongly whereas the LUMO would be stabilized moderately by the electron-withdrawing nitro group. This is consistent with the calculated orbital energy levels and then the HOMO−LUMO energy gap of **1a** becomes larger than that of **2a** (Figure 3). The smaller contribution of the C=N bond π-orbital in the tripentacyclic moiety (indicated by the arrows), which would be a key factor in unusually high HOMO energy levels in the N-fused porphyrin systems,[6,7] might be another factor of the relatively lower HOMO energy level in **1a**.

The blue-shifts in the *meso*-mesityl derivatives compared to the *meso*-phenyl derivatives observed in the absorption spectra could be explained by a loss of orbital interactions between the aryl group at the 5-position and the [18]-annulenic π-system in the N-fused porphyrin framework. The dihedral angles (ϕ_n) between the *meso*-aryl groups at the *n*-position (n = 5, 10, 15, 20) and the porphyrin mean plane composed of 24 heavy atoms are summarized in Table 2. In tetraphenylporphyrin (TPP), the dihedral angles are around 64° (entry 5). In contrast, the *meso*-mesityl groups are perpendicular to the porphyrin plane in tetramesitylporphyrin (TMP, entry 6). Nevertheless, the absorption wavelengths of TPP (645 nm) and TMP (646 nm) in CH_2Cl_2 are almost identical to each other. Meanwhile, in the case of NFTPP (**2a**), ϕ_5 (25.6°) is significantly smaller than the rest of the angles (entry 1). Accordingly, a large contribution of the 5-phenyl group is clearly observed in its HOMO and LUMO (Figure 2a,b). The contributions of the 10-, 15-, and 20-phenyl groups are comparatively small or negligible. Thus, the small ϕ_5 caused the facile electronic interaction between the 5-phenyl group and the N-fused porphyrin skeleton, which led to the red-shift in the absorption spectrum. The smaller ϕ_5 would be due to the smaller steric hindrance around the tripentacyclic moiety in the NFP framework. By changing the phenyl group to the mesityl group, the ϕ_5 becomes significantly larger (69.7°) because of the steric repulsion between the *o*-methyl groups and the β-hydrogen atoms of the pyrrole rings (entry 2). Accordingly, contribution of the 5-aryl ring in the HOMO and LUMO became negligible (Figure 2e,f). Then, compared to **2a**, the HOMO energy level is stabilized and the LUMO energy level is destabilized in **2g**, resulting in a significant blue-shift in the absorption spectrum. This trend is also observed in 21-NO_2-NFPs (entries 3 and 4). A considerable blue-shift in **1g** from **1a** could be rationalized by the larger ϕ_5.

Fluorescence Spectroscopy. The emission spectra of NFTPP derivatives were measured in CH_2Cl_2 at ambient temperature under Ar atmosphere. Representative emission spectra are shown in Figure 4 and the numerical data are summarized in Table 3. Unfortunately, the emission intensity of **2a** was very weak and its quantum yield could not be

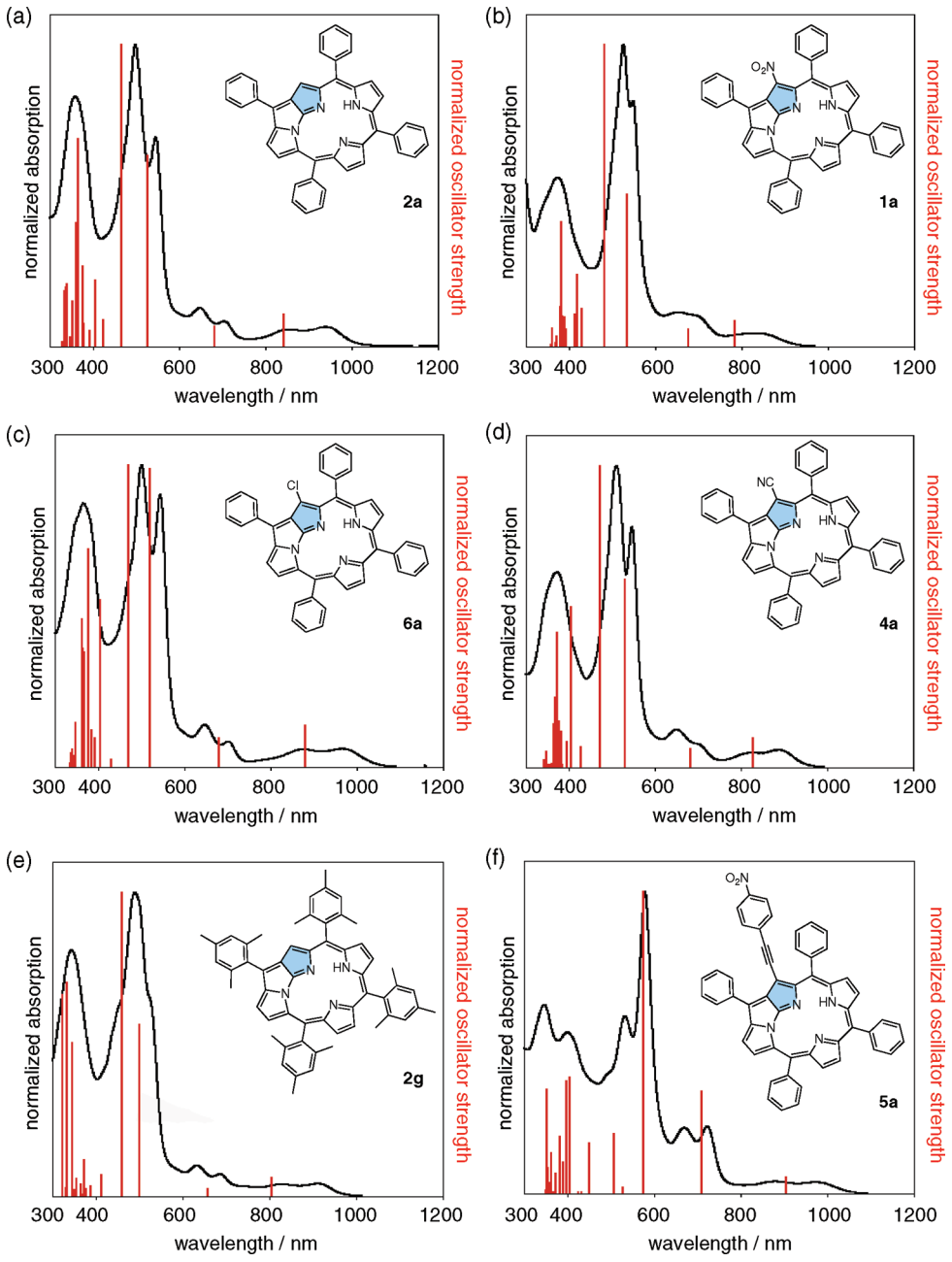

FIGURE 1. Absorption spectra and calculated oscillator strengths of (a) **2a**, (b) **1a**, (c) **6a**, (d) **4a**, (e) **2g**, and (f) **5a** at the B3LYP/6-311++G**//B3LYP/6-31G** level.

determined due to the background noise (entry 1). Essentially no emission was observed in **3a** and **6a** (entries 9 and 10) possibly due to the intramolecular heavy atom effect of the halogen atoms. However, a considerable refinement in the emission efficiency was observed through the introduction of a nitro group at the 21-position. For example, the emission quantum yield (Φ_{FL}) becomes $\Phi_{FL} = 2.7 \times 10^{-4}$ in **1a** (entry 2). The electron-donating groups in the *meso*-aryl positions cause further refinement of the emission quantum yields (entries 3−6) and it reaches $\Phi_{FL} = 5.0 \times 10^{-4}$ in **1d** (entry 5). Meanwhile, introduction of the electron-withdrawing groups in the *meso*-aryl positions causes a slight decrease to $\Phi_{FL} = 2.2 \times 10^{-4}$ (entry 7). The important features in the emission properties of 21-NO_2-NFPs are the large Stokes shifts (923−1261 cm^{-1}) compared to that of the parent NFTPP **2a** (402 cm^{-1}). The large Stokes shifts are quite intriguing and unusual for those kinds of rigid porphyrinic systems, which suggests a sizable structural change between the ground and excited states. In line with its absorption spectrum, the blue-shift from **1a** is observed in the emission spectrum of the mesityl derivative (**1g**) with a relatively small Stokes shift (923 cm^{-1}) among 21-NO_2-NFPs (entry 8). The cyano derivative **4a** shows similar emission properties to **1a** except for the smaller Stokes shift of 672 cm^{-1} (entry 11). The significant red-shift is observed in **5a**, where the extension of the π-conjugated system is expected, although the emission quantum yield becomes much lower ($\Phi_{FL} = 0.2 \times 10^{-4}$, entry 12). The origin of the fluorescence in NFTPPs is not clear at this moment, but the observed large Stokes shifts except for **2a** and the smaller fluorescence quantum yields suggest that the intramolecular proton transfer process would affect the

TABLE 1. Absorption Wavelengths of N-Fused Porphyrin Derivatives in CH_2Cl_2

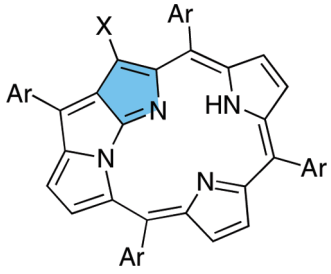

entry		Ar−	−X	λ_{max}/nm (log ε)							
1	**2a**	Ph−	−H	360 (4.59)		499 (4.68)	545 (4.52)	647 (3.78)	704 (3.60)	852 (3.42)	941 (3.50)
2	**2g**	2,4,6-Me_3-C_6H_2−	−H	344 (4.50)		489 (4.59)		633 (3.59)	687 (3.44)	828 (3.17)	911 (3.21)
3	**1a**	Ph−	$-NO_2$	374 (4.49)		526 (4.74)	548 (4.65)	651 (3.90)			837 (3.40)
4	**1b**	4-Me-C_6H_4−	$-NO_2$	384 (4.57)		527 (4.85)	554 (4.73)	656 (3.98)	701[b]		839 (3.58)
5	**1c**	4-^{t}Bu-C_6H_4−	$-NO_2$	384 (4.61)		527 (4.88)	554 (4.86)	658 (4.01)	702[b]		845 (3.61)
6	**1d**	4-MeO-C_6H_4−	$-NO_2$	339 (4.59)	404 (4.63)	529 (4.99)	561 (4.79)	664 (4.18)	703 (4.16)		850 (3.79)
7	**1e**	3,4,5-$(MeO)_3$-C_6H_2−	$-NO_2$	342 (4.59)		532 (4.91)	561 (4.75)	663 (4.06)	707[b]		854 (3.65)
8	**1f**	4-CF_3−C_6H_4−	$-NO_2$	368 (4.66)		529 (4.90)		688 (3.89)			833 (3.48)
9	**1g**	2,4,6-Me_3-C_6H_2−	$-NO_2$	350 (4.33)		528 (4.69)		683 (3.56)			825 (3.15)
10	**3a**	Ph−	−Br	368 (4.63)		500 (4.69)	542 (4.67)	646 (3.85)	699 (3.63)	868 (3.46)	957 (3.46)
11	**6a**	Ph−	−Cl	366 (4.65)		501 (4.71)	544 (4.66)	647 (3.85)	701 (3.63)	881 (3.47)	964 (3.48)
12	**5a**	Ph−	−CC-Ar′[a]	347 (4.70)	402 (4.63)	533 (4.69)	580 (4.94)	671 (4.28)	724 (4.29)	879 (3.52)	973 (3.52)
13	**4a**	Ph−	−CN	372 (4.69)		511 (4.88)	547 (4.77)	650 (3.98)	697[b]	828[b]	885 (3.64)

[a]Ar′− = 4-NO_2-C_6H_4−. [b]Shoulder.

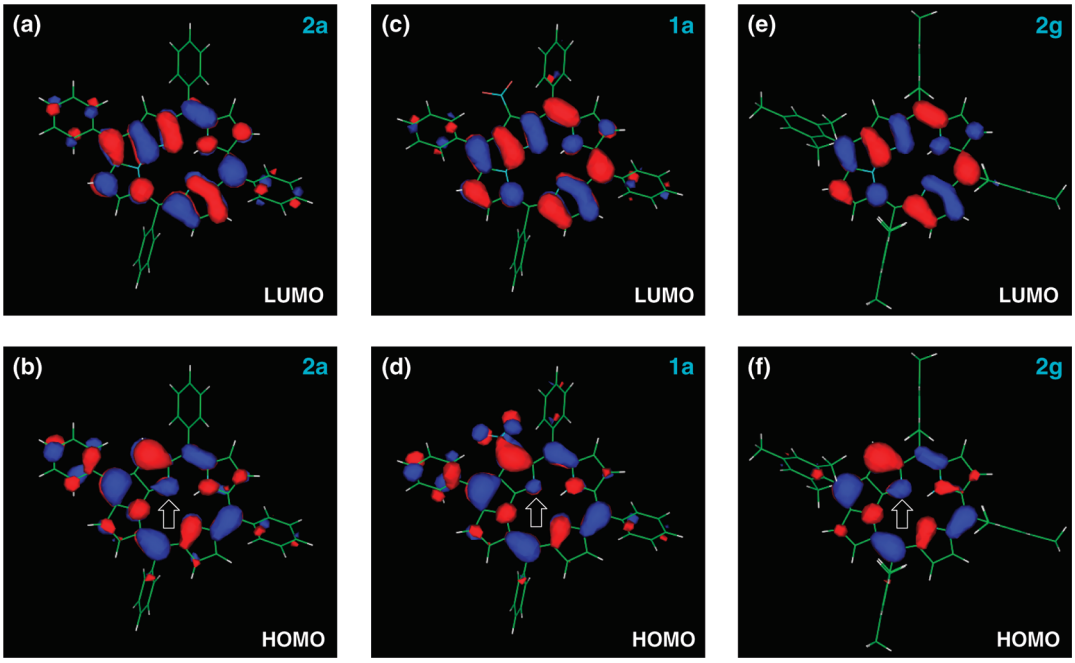

FIGURE 2. Kohn−Sham orbitals of **1a**, **2a**, and **2g**: (a) LUMO of **2a**, (b) HOMO of **2a**, (c) LUMO of **1a**, (d) HOMO of **1a**, (e) LUMO of **2g**, and (f) HOMO of **2g**. The arrows indicate the C=N bond in the tripentacyclic moiety.

excited-state dynamics, especially the fluorescence emission behavior. The excited-state intramolecular proton transfer (ESIPT) process occurs generally when acidic and basic moieties exist in proximity within the same molecule,[11] and this process is further facilitated by the intramolecular hydrogen bonding. Depending upon the molecular systems, the ESIPT state is generally characterized either by radiative or nonradiative decay pathways. In the NFTPP derivatives, the ESIPT process would be observed by virtue of proton transfer from the N(24) atom to the N(2) atom in the excited state. The feasible mechanism for the ESIPT process and the influence of substituents are discussed separately.

Excited State Intramolecular Proton Transfer (ESIPT). The fluorescent properties of NFPs and the role of substituents on the emission quantum yields could be rationalized by the tailored efficiency of the ESIPT process. ESIPT is a

(11) (a) Tolbert, L. M.; Solntsev, K. M. *Acc. Chem. Res.* **2002**, *35*, 19. (b) Waluk, J. *Acc. Chem. Res.* **2006**, *39*, 945. (c) Hsieh, C.-C.; Jiang, C.-M.; Chou, P.-T. *Acc. Chem. Res.* **2010**, *43*, 1364. (d) Agmon, N. *J. Phys. Chem. A* **2005**, *109*, 13. (e) Petrich, J. W. *Int. Rev. Phys. Chem.* **2000**, *19*, 479.

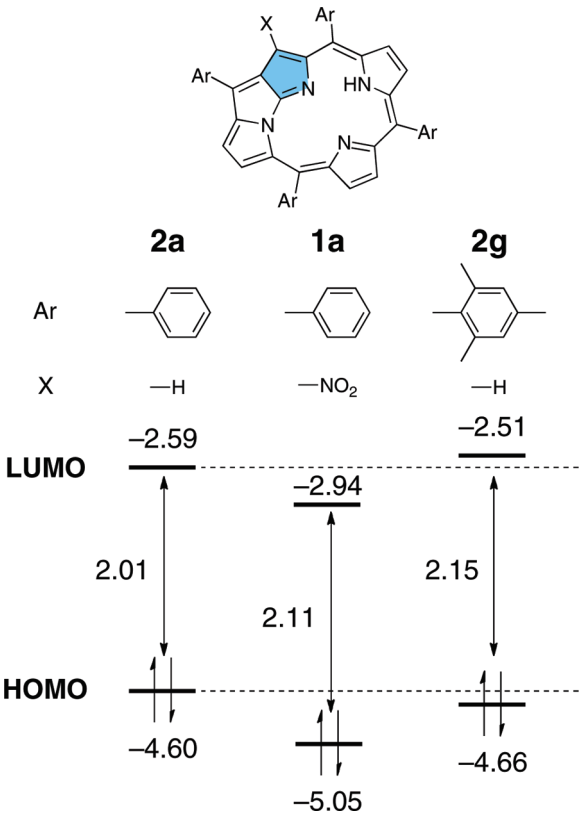

FIGURE 3. Orbital energy levels of **1a**, **2a**, and **2g**.

kind of phototautomerism that occurs at the excited state of the molecule. Incidentally, there could exist three NH tautomers in the NFPs (Chart 2), where **NFP−A** would be dominant in solution because of its thermodynamic stability (Table 4). The energy difference between **NFP−A** and **NFP−B** is small (ca. 2.5 kcal/mol) and may play a negligible role in emission efficiency. In contrast, the energy difference between **NFP−A** and **NFP−C** was calculated to be 6−9 kcal/mol and depends much on the substituents. The relatively large energy difference suggests a negligible contribution of **NFP−C** in the ground state; however, **NFP−C** would contribute significantly in the excited state. In this context, the excited state tautomerism between **NFP−A** (or **NFP−B**) and **NFP−C** is assumed to be important in depicting the radiative and nonradiative decay process. Thus, we believe that ESIPT is responsible for the observed emission in NFPs because fluorescence from the singlet excited state of porphyrinic systems generally has not been accompanied by larger Stokes shift values due to their rigid planar structures. Being with the rigid structures, the observed Stokes shifts ($\sim$1200 cm^{-1}) for NFPs are quite unusual and probably due to the phototautomerism from **NFP−A** (or **NFP−B**) to **NFP−C** in the excited state. In contrast, removal of protons by *N*-methylation of nitrogen at the 24-position (vide infra) or by double N-fusion hampered the fluorescence emission.[6,12] The ESIPT process in NFPs would be induced by the presence of intramolecular hydrogen bonding between the acidic N(24)H moiety and the basic N(2) atom in the ground state. The charge density distribution changes upon excitation and the consequent changes in the intramolecular hydrogen bonding between the acidic and basic centers are the driving force for the ESIPT process.[13] Indeed, the geometry optimized for **1a** suggests the strong intramolecular hydrogen bonding between the N(24)H moiety and the N(2) atom inside the NFP macrocycle (Figure 5). Further insights in this regard would be gleaned from the ^{1}H NMR chemical shifts of the NH protons inside the macrocycle. A signal due to the NH proton of NFPs is usually observed in the region of 5−9 ppm. This feature is in sharp contrast with regular porphyrins, where the signal due to the NH protons inside the macrocycle is observed in the high-field region (−3 to −2 ppm). It should be noted that both regular and N-fused porphyrins possess strong aromaticity, where a strong shielding effect is expected inside the macrocycle. Thus, the signals due to the inner NH proton of NFPs appear in the unexpectedly low-field region. This can be explained by the strong intramolecular hydrogen bonding between the N(24)H moiety and the N(2) atom inside the NFP macrocycles. The low-field shift of the inner NH proton signal means strong N(2)−HN(24) interaction, which implies the facile NH tautomerization from **NFP−A** to **NFP−C**. Thus, based on the above facts, we can conclude that the observed fluorescence emission from the NFTPP derivatives originates from the ESIPT state (S_1'), which can be explained by using Figure 6. Upon excitation, the molecule in the excited singlet state undergoes radiationless proton transfer to the ESIPT state ($S_1 \rightarrow S_1'$), followed by $S_1' \rightarrow S_0'$ fluorescence and then reverse proton transfer to the normal tautomer in the ground state ($S_0' \rightarrow S_0$). The prime ($'$) indicates the ground and excited states for the **NFP−C** tautomer.

We have also measured the transient absorption spectra of **1a** using femtosecond pulses (Figure 7) to obtain further insights for the ESIPT process. The transient absorption spectra show the ground state bleaching signals at 525 and 550 nm along with the excited-state absorptions at 475 and 595 nm. Although the transient absorption spectra of **1a** show two distinct ground-state bleaching signals, the excited-state dynamics of **1a** reveal monoexponential behavior with a 13.5 ps time component in all the spectral regions. Previously, the fast decay dynamics in fused porphyrinoids were observed. The excited-state lifetime of **2a** was unusually short (10.6 ps) and even shorter than that of doubly N-fused porphyrin possessing the narrower HOMO−LUMO gap ($\sim$20 ps).[12] Although both compounds have the rigid frameworks, only the former has the NH moiety inside the macrocycle. On the basis of this observation, the inner NH moiety of the **1a** and **2a** would be a key factor of their unusually ultrafast excited-state lifetime. In other words, the ESIPT process among the inner NH and N moieties is strongly related to its fast relaxation dynamics and unique NIR fluorescence behaviors of NFPs.

In contrast to the nitro-substituted NFPs, the too small Stokes shift value for the parent compound **2a** (402 cm^{-1}) is not fully understood at this moment. The relatively small energy difference between the tautomers **NFP−A** (or **NFP−B**) and **NFP−C** may be responsible for this feature. Direct emission from the S_1 state is another possibility.

(12) Lee, J. S.; Lim, J. M.; Toganoh, M.; Furuta, H.; Kim, D. *Chem. Commun.* **2010**, *46*, 285.

(13) (a) Formosinho, S. J.; Arnaut, L. G. *J. Photochem. Photobiol., A* **1993**, *75*, 21. (b) Doroshenko, A. O.; Posokhov, E. A.; Verezubova, A. A.; Ptyagina, L. M.; Skripkina, V. T.; Shershukov, V. M. *Photochem. Photobiol. Sci.* **2002**, *1*, 92.

TABLE 2. The Dihedral Angles (ϕ_n) between the *meso*-Aryl Groups and the Porphyrin Mean Plane

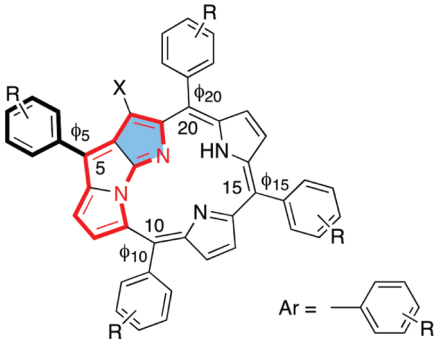

entry		Ar−	−X	ϕ_5 (deg)	ϕ_{10} (deg)	ϕ_{15} (deg)	ϕ_{20} (deg)	$\lambda_{abs}{}^a$ (nm)
1	**2a**	Ph−	−H	25.6	75.6	52.9	55.4	941
2	**2g**	2,4,6-Me_3-C_6H_2−	−H	69.7	89.2	89.3	89.8	911
3	**1a**	Ph−	$-NO_2$	41.6	79.0	55.5	60.3	835
4	**1g**	2,4,6-Me_3-C_6H_2−	$-NO_2$	74.7	89.1	87.4	84.0	818
5	TPP	Ph−		64.3	64.3	64.1	64.2	645
6	TMP	2,4,6-Me_3-C_6H_2−		90.1	90.0	89.9	90.1	646

[a]The longest λ_{max} in CH_2Cl_2.

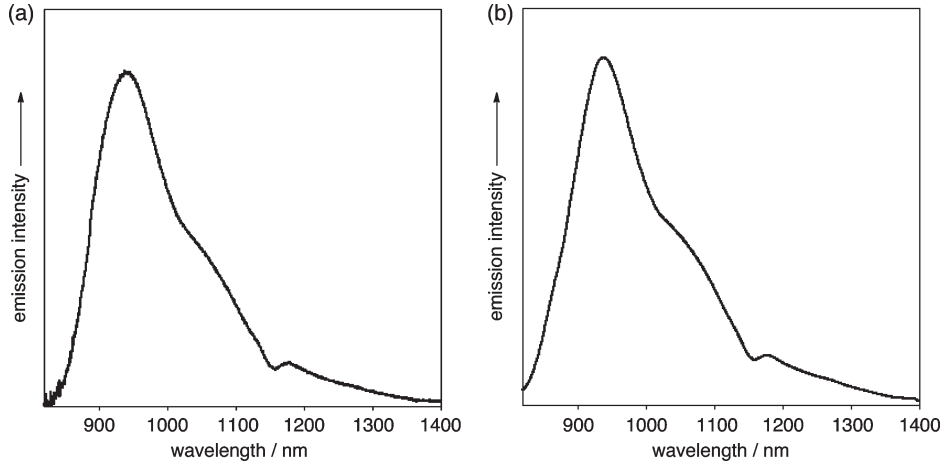

FIGURE 4. Emission spectra of (a) **1c** and (b) **4a** in CH_2Cl_2.

TABLE 3. The Fluorescence Properties of the N-Fused Porphyrin Derivatives in CH_2Cl_2

entry		Ar−	−X	λ_{abs} (nm)	λ_{FL} (nm)	Φ_{FL} ($\times 10^{-4}$)	Stokes shift (cm^{-1})
1	**2a**	Ph−	−H	941	978	< 0.1	402
2	**1a**	Ph−	$-NO_2$	837	930	2.7	1195
3	**1b**	4-Me-C_6H_4−	$-NO_2$	839	937	3.0	1247
4	**1c**	4-^{t}Bu-C_6H_4−	$-NO_2$	845	944	3.5	1241
5	**1d**	4-MeO-C_6H_4−	$-NO_2$	850	952	5.0	1261
6	**1e**	3,4,5-$(MeO)_3C_6H_2$−	$-NO_2$	854	950	3.2	1183
7	**1f**	4-CF_3−C_6H_4−	$-NO_2$	833	917	2.2	1100
8	**1g**	2,4,6-Me_3-C_6H_2−	$-NO_2$	825	893	2.9	923
9	**3a**	Ph−	−Br	957	−[b]	−[b]	−[b]
10	**6a**	Ph−	−Cl	964	−[b]	−[b]	−[b]
11	**4a**	Ph−	−CN	885	941	2.8	672
12	**5a**	Ph−	−CC-Ar′[a]	973	1050	0.2	754

[a]Ar′− = 4-NO_2-C_6H_4−. [b]Not detected.

However, detailed spectroscopic studies are needed to understand the phenomena completely.

Fluorescence quantum yields of NFPs are highly sensitive to the substituents on the *meso*-phenyl ring (ϕ_5). This substituent effect can be explained by the influence of the electron-donating or -withdrawing nature of the substituents on the relative electron density of the N(24) atom. In this regard, we have plotted the fluorescence quantum yields of the para-substituted 21-NO_2-NFTPP derivatives (**1a**−**d** and **1f**) in logarithmic scale against the electron-donating/withdrawing strength of the substituents in terms of Yukawa and Tsuno's constant (σ_π).[14] The plot shows a good linear

CHART 2. NH Tautomers of NFPs

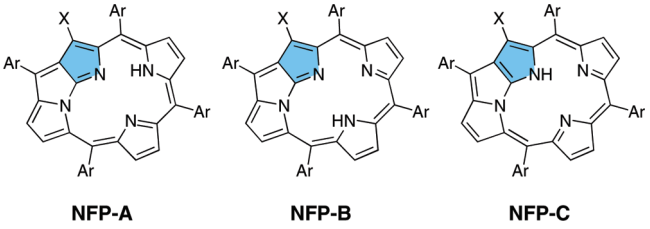

relationship with a negative slope (correlation coefficient $r = 0.95$), so that as σ_π increases, Φ_{FL} decreases, i.e. the fluorescence quantum yield decreases with increasing electron-withdrawing strength of the substituents (Figure 8). Electron-withdrawing substituents decrease the basicity of the N(24) atom and hence its proton affinity, thus leading to the small fluorescence quantum yields.

Solvent Effects. The photophysical properties of **1a** and **2a** were measured in a variety of solvents and summarized with empirical solvent polarity scales (E_T^N) in Table 5.[15] While the absorption wavelengths of **2a** are nearly insensitive to the solvents, considerable blue-shifts with increase in the polarity of the solvents are observed for **1a**. Interestingly, the emission wavelengths of **1a** are nearly insensitive to the solvents in spite of the significant solvent dependency in the absorption spectra. This implies the negative solvatochromism, where the ground states are stabilized relative to the excited state. This feature is quite consistent with the larger contribution of the nitro group in HOMO. Increase of the solvent polarity develops the zwitterionic character on the nitro group and shows larger dipole moment changes in the ground state than the excited state. The overall effect is an increase of the HOMO−LUMO energy gap. A slight refinement of the emission quantum yields of **1a** in different solvents might be explained by interplay between the energy gap law and solvent polarity. While the photophysical properties of nonplanar porphyrins such as dodecaphenylporphyrin show unique solvent dependency due to the interactions of solvent molecules with the inner NH protons, those of planar porphyrins are insensitive to the solvents.[16] Since both **1a** and **2a** have the planar conformations, such solvent effect would not be important in the case of NFPs.[5] It should be noted that the relatively small solvents effect discussed here would indicate negligible contribution of the intramolecular electron transfer process in emission decay of NFP.

***N*-Methylation.** To disturb the NH tautomerization, *N*-methylation reactions of NFP were achieved. Although the reaction of **2a** with MeI did not proceed efficiently, the reaction of **2a** with $MeOSO_2CF_3$ afforded an *N*-methyl N-fused tetraphenylporphyrinium salt $\mathbf{11aH^+ \cdot OSO_2CF_3^-}$ in 73% yield. The *N*-methylation reaction proceeded regioselectively and only the single isomer was obtained, which was confirmed by the ^{1}H NMR and X-ray crystallographic analyses (Figure 9).[17] Unexpectedly $\mathbf{11aH^+ \cdot OSO_2CF_3^-}$ was very stable and an attempt to isolate a neutral form of **11a** by treatment with a base has so far been unsuccessful. Interestingly no fluorescence could be detected for $\mathbf{11aH^+ \cdot OSO_2CF_3^-}$. This observation is quite consistent with our interpretation that the observed fluorescence emission from NFPs is due to the excited state intramolecular proton transfer. Evidently, molecular distortion imposed by the *N*-methyl group could affect fluorescence efficiency, since the *N*-methylated pyrrole ring plane calculated from the 5 heavy atoms was tilted by 48.0° from the NFP plane composed of the rest of the 19 heavy atoms in $\mathbf{11aH^+ \cdot OSO_2CF_3^-}$. Although no clear evidence was obtained yet, the effect of molecular distortion would not be a critical issue, because distinctive fluorescence was observed in the case of *N*-methylated porphyrins.[18] It should be noted that the distinct fluorescence was observed in $\mathbf{1aH^+}$, where ESIPT between the N(24)H moiety and the N(2) atom is still expected, since protonation would occur preferentially at the N(23) atom.[12,19]

Conclusion

A variety of NFP derivatives were synthesized and their absorption as well as emission properties were investigated. Although the emission quantum yields are not so high, the NFP derivatives showed the distinct fluorescence in the near-infrared region (900−1000 nm). Since the NFPs have the relatively small π-systems, namely, the [18]annulenic circuit, these are interesting examples among near-infrared emissive organic materials. The large Stokes shifts ($\sim$1200 cm^{-1}), the weak emission quantum yields ($\sim 5.0 \times 10^{-4}$), and the unusually short S_1 state lifetimes ($\sim$13.5 ps) indicate that the fluorescence emission from NFPs is due to ESIPT, which is a rare example among near-infrared emissive dyes. This study demonstrates that the ring-fusion strategy is an effective way to produce organic materials possessing unique photophysical properties. Combined with coordination chemistry of NFPs,[20] further studies on the photophysical properties of N-fused porphyrinoids including the detailed excited state dynamics of the proton transfer process as well as their applications in the field of materials science are now in progress.

Experimental Section

General. All the reactions were performed in oven-dried reaction vessels under Ar or N_2. Commercially available solvents and reagents were used without further purification unless otherwise mentioned. *N*-bromosuccinimide was recrystallized

(14) (a) Yukawa, Y.; Tsuno, Y. *Bull. Chem. Soc. Jpn.* **1959**, *32*, 971. (b) Tsuno, Y.; Fujio, M. *Chem. Soc. Rev.* **1996**, *25*, 129. (c) Nagaoka S.; Nakamura, A.; Nagashima, U. *J. Photochem. Photobiol., A* **2002**, *154*, 23.

(15) Reichardt, C. *Chem. Rev.* **1994**, *94*, 2319.

(16) Takeda, J.; Sato, M. *Chem. Lett.* **1995**, *24*, 971.

(17) Crystal data: $\mathbf{11aH^+ \cdot OSO_2CF_3^-}$, violet platelet, $C_{46}H_{31}F_3N_4O_3S$, M_W 776.81, triclinic, space group $P\bar{1}$ (No. 2), $a = 10.1624(10)$ Å, $b = 14.6757(15)$ Å, $c = 15.1354(15)$ Å, $\alpha = 83.821(2)°$, $\beta = 76.625(2)°$, $\gamma = 70.557(2)°$, $V = 2069.7(4)$ Å^3, $Z = 2$, $T = 223(2)$ K, $R = 0.0795$ ($I > 2\sigma(I)$), $R_W = 0.2372$ (all data), GOF = 0.814. The crystallographic coordinates have been deposited with the Cambridge Crystallographic Data Centre; deposition no. 790805. These data can be obtained free of charge from the Cambridge Crystallographic Data Centre, 12 Union Rd., Cambridge CB2 1EZ, UK or via www.ccdc.cam.ac.uk/conts/retrieving.html.

(18) (a) Sazanovich, I. V.; Berezin, D. B.; van Hoek, A.; Panarin, A. Y.; Bolotin, V. L.; Semeykin, A. S.; Chirvony, V. S. *J. Porphyrins Phthalocyanines* **2005**, *9*, 59. (b) Shkirman, S. F.; Solov'ev, K. N.; Kachura, T. F.; Arabei, S. A.; Skakovskii, E. D. *J. Appl. Spectrosc.* **1999**, *65*, 68.

(19) Ikawa, Y.; Harada, H.; Toganoh, M.; Furuta, H. *Bioorg. Med. Chem. Lett.* **2009**, *19*, 2448.

(20) (a) Toganoh, M.; Ishizuka, T.; Furuta, H. *Chem. Commun.* **2004**, 2464. (b) Toganoh, M.; Ikeda, S.; Furuta, H. *Inorg. Chem.* **2007**, *46*, 10003. (c) Młodzianowska, A.; Latos-Grażyński, L.; Szterenberg, L.; Stępień, M. *Inorg. Chem.* **2007**, *46*, 6950. (d) Młodzianowska, A.; Latos-Grażyński, L.; Szterenberg, L. *Inorg. Chem.* **2008**, *47*, 6364. (e) Toganoh, M.; Ikeda, S.; Furuta, H. *Chem. Commun.* **2005**, 4589. (f) Toganoh, M.; Fujino, K.; Ikeda, S.; Furuta, H. *Tetrahedron Lett.* **2008**, *49*, 1488. (g) Skonieczny, J; Latos-Grażyński, L.; Szterenberg, L. *Inorg. Chem.* **2009**, *48*, 7394.

TABLE 4. The Relative Energies of the NFP Tautomers Calculated at the B3LYP/6-31G Level**

						rel energies (kcal/mol)		
entry		Ar−	−X	Φ_{FL} ($\times10^{-4}$)	δ_{NH}	**NFP−A**	**NFP−B**	**NFP−C**
1	**2a**	Ph−	−H	<0.1	8.52	0.00	2.19	6.57
2	**1a**	Ph−	$-NO_2$	2.7	5.56	0.00	2.74	9.13
3	**1d**	4-MeO-C_6H_4−	$-NO_2$	5.0	5.48	0.00	2.60	9.22
4	**1f**	4-CF_3-C_6H_4−	$-NO_2$	2.2	5.42	0.00	2.86	9.11
5	**1g**	2,4,6-Me_3-C_6H_2−	$-NO_2$	2.9	5.94	0.00	3.09	8.80
6	**4a**	Ph−	−CN	2.8	6.36	0.00	2.73	8.85
7	**5a**	Ph−	−CC-Ar′[a]	0.2	7.49	0.00	1.10	6.94

[a]Ar′− = 4-NO_2-C_6H_4−.

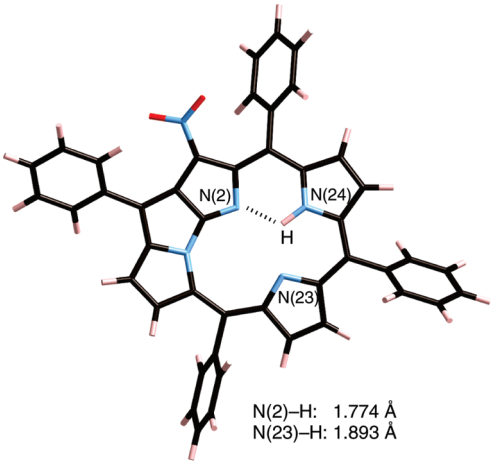

FIGURE 5. Intramolecular hydrogen bonding in **1a**. The structure was optimized with the B3LYP/6-31G** level calculation.

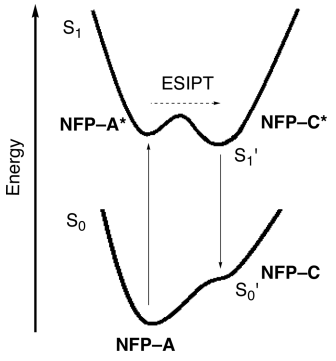

FIGURE 6. Excited state intramolecular proton transfer process in NFP. **NFP−A** and **NFP−C** are in the ground state and **NFP−A*** and **NFP−C*** are in the excited state.

from hot water. Thin-layer chromatography (TLC) was carried out on aluminum sheets coated with silica gel 60 F_{254} (MERCK). Preparative separation was performed by silica gel flash column chromatography (KANTO Silica Gel 60 N, spherical, neutral, 40−50 μm) or silica gel gravity column chromatography (KANTO Silica Gel 60 N, spherical, neutral, 63-210 μm). ^{1}H NMR spectra were recorded in $CDCl_3$ solution at 300 MHz and chemical shifts were reported relative to a residual proton of a deuterated solvent, $CHCl_3$ (δ = 7.26) in ppm. ^{13}C NMR spectra were recorded at 75 MHz and chemical shifts were reported relative to $CDCl_3$ (δ = 77.00) in ppm. UV/vis/NIR absorption spectra were recorded with a photomultiplier tube detector (190−750 nm) and a PbS detector (750−3200 nm). Mass spectra were recorded on a MALDI−TOF−MS spectrometer. High-resolution mass spectra were measured with a ESI−MS spectrometer. Emission spectra were recorded with an InGaAs photodiode detector. A sensitivity

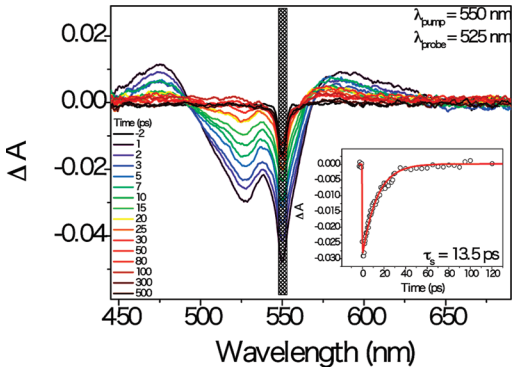

FIGURE 7. Transient absorption spectra of **1a** pumped at 550 nm. The inset shows decay of signal probed at 525 nm.

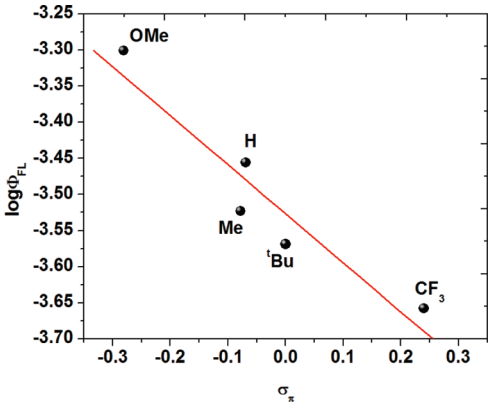

FIGURE 8. Plots of log Φ_{FL} against σ_π for the 21-NO_2-NFP derivatives (**1a**−**d**,**f**). The red line shows the regression line.

TABLE 5. The Solvent Effect on the Photophysical Properties of 1a and 2a

			1a			**2a**
entry	solvent	E_T^N [a]	λ_{ABS} (nm)	λ_{FL} (nm)	Φ_{FL} ($\times10^{-4}$)	λ_{ABS} (nm)
1	cyclohexane	0.006	862	936	2.2	939
2	toluene	0.099	850	932	2.4	937
3	CH_2Cl_2	0.309	837	932	2.7	941
4	DMF	0.386	840	930	3.0	942
5	MeOH	0.762	828	927	3.3	944

[a]Reference 15.

correction function implementation was applied for all the emission spectra. Emission efficiency was based on the integral intensity of the emission spectra relative to IR-1040.[21] The integral intensities are reproducible and representative errors are less than

(21) Casalboni, M.; De Matteis, F.; Prosposito, P.; Quatela, A.; Sarcinelli, F. *Chem. Phys. Lett.* **2003**, *373*, 372.

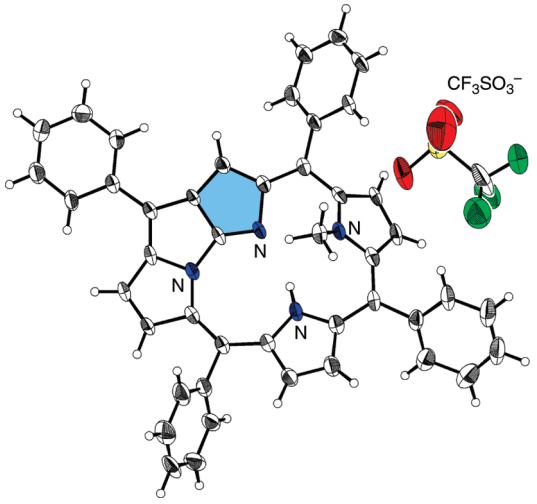

FIGURE 9. X-ray structure of **11aH**$^+$·**OSO$_2$CF$_3$**$^-$. The thermal ellipsoids are shown at the 30% probability level.

10%. **1b**,[5b] **2a**,[5b] **3a**,[5b] **4a**,[7b] **5a**,[9] **6a**,[5b] **7a**−**f**,[22] **7g**,[23] **8a**,[8a] and **10a**[5] were prepared according to the reported procedures. Since complete removal of solvents from samples without decomposition was quite difficult, elemental analyses were usually achieved with the samples containing CH_2Cl_2. The samples were dried under vacuum overnight under gentle heating and the amounts of remaining CH_2Cl_2 were checked by ^{1}H NMR analysis.

Femtosecond Transient Absorption Measurements. The femtosecond time-resolved transient absorption (TA) spectrometer was pumped by a Ti:sapphire regenerative amplifier system operating at 1 kHz repetition rate and an optical detection system. The frequency doubled 400 nm pulses had a pulse width of ∼100 fs and an average power of 1 mW, which were used as pump pulses. White light continuum (WLC) probe pulses were generated with use of a sapphire window (2 mm of thickness) by focusing a small portion of the fundamental 800 nm pulses. The time delay between pump and probe beams was carefully controlled by making the pump beam travel along a variable optical delay. Intensities of the spectrally dispersed WLC probe pulses are monitored by a miniature spectrograph. To obtain the time-resolved transient absorption difference signal (ΔA) at a specific time, the pump pulses were chopped at 25 Hz and absorption spectra intensities were saved alternately with or without pump pulse. Typically, 6000 pulses excite samples to obtain the TA spectra at a particular delay time. The polarization angle between pump and probe beam was set at the magic angle (54.7°) in order to prevent polarization-dependent signals. Cross-correlation fwhm in pump−probe experiments was less than 200 fs and the chirp of WLC probe pulses was measured to be 800 fs in the 400−800 nm regions. To minimize chirp, all reflection optics in the probe beam path and 2 mm path length of the quartz cell were used. The three-dimensional data sets of ΔA versus time and wavelength were subjected to singular value decomposition and global fitting to obtain the kinetic time constants and their associated spectra using Surface Xplorer software.

General Procedures for Nitration of NCP (7). An aqueous hydrochloric acid solution (3.3 wt %, 200 mL) of sodium nitrite (2 g) was mixed with a dichloromethane solution (50 mL) of **7** (200 mg). The resulting slurry was vigorously stirred at room temperature for 1 min. After the reaction mixture was neutralized with Na_2CO_3, the organic layer was separated, filtered through a pad of Na_2SO_4, and concentrated under reduced pressure. The residue was separated by a silica gel column with CH_2Cl_2. Collection of the first green band followed by recrystallization with CH_2Cl_2/hexane afforded **8**.

21-Nitro N-confused 5,10,15,20-tetrakis(4-methylphenyl)-porphyrin (8b): 131 mg (0.184 mmol, 62% yield); ^{1}H NMR ($CDCl_3$, 300 MHz, ppm) δ −3.78 (br s, 2H), 2.69 (s, 3H), 2.70 (s, 6H), 2.72 (s, 3H), 7.54−7.59 (m, 4H), 7.69−7.73 (m, 4H), 7.96−7.98 (m, 1H), 8.01−8.04 (m, 2H), 8.05 (s, 1H), 8.09−8.12 (m, 1H), 8.34 (d, J = 7.8 Hz, 4H), 8.57 (d, J = 4.9 Hz, 1H), 8.60 (d, J = 4.9 Hz, 1H), 8.77 (d, J = 4.9 Hz, 2H), 9.17 (d, J = 5.1 Hz, 1H), 9.20 (d, J = 5.1 Hz, 1H); ^{13}C NMR ($CDCl_3$, 75 MHz, ppm) δ 21.50, 21.55, 21.57, 114.75, 121.81, 122.54, 127.50, 127.83, 128.00, 128.65, 128.87, 128.97, 129.05, 129.17, 129.42, 130.83, 134.54, 134.71, 134.89, 135.08, 135.82, 136.05, 136.16, 137.61, 137.76, 137.91, 137.95, 138.01, 138.17, 138.34, 138.40, 138.86, 139.63, 140.64, 140.91, 141.28, 141.39, 142.74, 152.41, 157.97, 158.71; MS (MALDI) m/z 715.51 ([M]$^+$), 669.51 ([M − NO_2]$^+$); HRMS (ESI$^+$) found m/z 716.30255, calcd for $C_{48}H_{38}N_5O_2$ (MH$^+$) m/z 716.30218; UV−vis−NIR (CH_2Cl_2, λ_{max}/nm (log ε)) 701 (4.42), 657 (4.37), 473 (5.39), 374 (4.86).

21-Nitro N-confused 5,10,15,20-tetrakis(4-*tert*-butylphenyl)-porphyrin (8c): 145 mg (0.164 mmol, 69% yield); ^{1}H NMR ($CDCl_3$, 300 MHz, ppm) δ −3.44 (br s, 2H), 1.65 (s, 36H), 7.81−7.85 (m, 4H), 7.99 (d, J = 8.5 Hz, 4H), 8.07−8.10 (m, 2H), 8.13−8.17 (m, 2H), 8.24 (d, J = 7.3 Hz, 1H), 8.45−8.50 (m, 4H), 8.64 (d, J = 4.9 Hz, 1H), 8.66 (d, J = 4.9 Hz, 1H), 8.88 (d, J = 4.9 Hz, 2H), 9.27 (d, J = 5.1 Hz, 1H), 9.32 (d, J = 5.1 Hz, 1H); ^{13}C NMR ($CDCl_3$, 75 MHz, ppm) δ 31.54, 31.56, 31.64, 34.93, 34.98, 35.05, 114.22, 121.86, 122.49, 123.67, 123.70, 124.04, 125.27, 128.11, 128.71, 128.79, 129.21, 129.48, 130.80, 134.44, 134.64, 134.91, 135.13, 135.91, 136.08, 137.55, 137.73, 137.95, 138.29, 138.38, 140.54, 140.98, 141.03, 141.31, 142.88, 151.03, 151.06, 151.60, 152.57, 158.11, 158.75; MS (MALDI) m/z 837.51 ([M − NO_2]$^+$); HRMS (ESI$^+$) found m/z 884.48967, calcd for $C_{60}H_{62}N_5O_2$ (MH$^+$) m/z 884.49035; UV−vis−NIR (CH_2Cl_2, λ_{max}/nm (log ε)) 702 (4.38), 659 (4.35), 474 (5.31), 375 (4.79).

21-Nitro N-confused 5,10,15,20-tetrakis(4-methoxyphenyl)-porphyrin (8d): 164 mg (0.200 mmol, 74% yield); ^{1}H NMR ($CDCl_3$, 300 MHz, ppm) δ −3.35 (br, 2H), 4.11 (s, 9H), 4.13 (s, 3H), 7.31−7.34 (m, 4H), 7.48−7.50 (m, 4H), 8.05 (d, J = 8.2 Hz, 1H), 8.07 (s, 1H), 8.11 (d, J = 8.9 Hz, 2H), 8.20 (d, J = 8.2 Hz, 1H), 8.44 (d, J = 4.0 Hz, 2H), 8.47 (d, J = 4.0 Hz, 2H), 8.61 (d, J = 4.9 Hz, 1H), 8.63 (d, J = 4.9 Hz, 1H), 8.82 (d, J = 4.9 Hz, 2H), 9.21 (d, J = 4.9 Hz, 1H), 9.24 (d, J = 4.9 Hz, 1H); ^{13}C NMR ($CDCl_3$, 75 MHz, ppm) δ 55.56, 55.60, 55.67, 112.46, 113.89, 113.94, 115.00, 121.29, 121.98, 127.84, 128.42, 128.48, 129.04, 129.28, 130.37, 133.46, 133.69, 133.78, 134.08, 135.65, 135.71, 135.82, 135.91, 136.21, 136.35, 136.42, 139.19, 139.35, 140.71, 141.11, 141.29, 141.47, 142.86, 152.68, 158.15, 158.84, 159.66, 159.68, 160.55, 161.09; MS (MALDI) m/z 778.45 ([M]$^+$), 733.45 ([M − NO_2]$^+$); UV−vis−NIR (CH_2Cl_2, λ_{max}/nm (log ε)) 708 (4.55), 674 (4.46), 479 (5.43), 384 (4.86). Anal. Calcd for **8d**·0.05CH_2Cl_2 ($C_{48.05}H_{37.1}Cl_{0.1}N_5O_6$): C, 73.60; H, 4.77; N, 8.93. Found: C, 73.49; H, 4.82; N, 8.91.

21-Nitro N-confused 5,10,15,20-tetrakis(3,4,5-trimethoxyphenyl)-porphyrin (8e): 131 mg (0.128 mmol, 63% yield); ^{1}H NMR ($CDCl_3$, 300 MHz, ppm) δ −3.47 (br, 2H), 3.93 (s, 3H), 3.96 (s, 3H), 4.00 (s, 3H), 4.04 (s, 3H), 4.12 (s, 6H), 4.14 (s, 6H), 4.16 (s, 3H), 4.17 (s, 6H), 4.20 (s, 3H), 7.29 (s, 1H), 7.38 (s, 1H), 7.40 (s, 1H), 7.50 (s, 1H), 7.66−7.70 (m, 4H), 8.19 (s, 1H), 8.65 (d, J = 4.9 Hz, 1H), 8.68 (d, J = 4.9 Hz, 1H), 8.87 (s, 1H), 8.89 (s, 1H), 9.22 (d, J = 4.9 Hz, 1H), 9.29 (d, J = 4.9 Hz, 1H); ^{13}C NMR ($CDCl_3$, 75 MHz, ppm) δ 56.34, 56.37, 56.46, 56.52, 56.57, 56.72, 61.14, 61.29, 61.35, 112.55, 112.71, 112.91, 113.05, 114.85, 115.47, 115.78, 121.39, 122.14, 128.07, 128.73, 129.01, 129.37, 129.72, 130.91, 135.98, 136.01, 136.20, 136.29, 136.47, 136.54, 136.60, 138.10, 138.12, 139.23, 139.79, 140.48, 140.89, 141.11, 141.32, 142.86, 151.48, 151.50, 151.55, 151.58, 152.33, 152.68, 152.77, 158.11, 158.90, 161.49, 162.45; MS (MALDI) m/z 778.45 ([M]$^+$), 733.45 ([M − NO_2]$^+$);

(22) Geier, G. R. III; Haynes, D. M.; Lindsey, J. S. *Org. Lett.* **1999**, *1*, 1455.
(23) Geier, G. R., III; Lindsey, J. S. *J. Org. Chem.* **1999**, *64*, 1596.

UV−vis−NIR (CH_2Cl_2, λ_{max}/nm (log ε)) 704 (4.21), 660 (4.16), 483 (5.22), 378 (4.60). Anal. Calcd for **8e**·0.3CH_2Cl_2 ($C_{56.3}H_{53.6}Cl_{0.6}N_5O_{14}$): C, 64.68; H, 5.17; N, 6.70. Found: C, 64.89; H, 5.12; N, 6.66.

General Procedures for Bromination of 21-NO_2-NCP (8). To a solution of **8** (1.0 equiv) in CH_2Cl_2 was added NBS (1.1 equiv), and the reaction mixture was stirred for 5 min at ambient temperature. The resulting mixture was directly poured on a silica gel column, which was eluted with CH_2Cl_2 to give **9**.

3-Bromo-21-nitro N-confused 5,10,15,20-tetraphenylporphyrin (9a): Starting from **8a** (100 mg, 0.152 mmol) in 20 mL of CH_2Cl_2, **9a** was obtained in 68% yield (77 mg, 0.104 mmol). ^{1}H NMR ($CDCl_3$, 300 MHz, ppm) δ −3.05 (br, 2H), 7.79−7.84 (m, 7H), 7.88−7.93 (m, 5H), 8.03−8.05 (m, 1H), 8.12−8.14 (m, 2H), 8.25−8.28 (m, 1H), 8.47−8.51 (m, 6H), 8.69−8.70 (m, 2H), 9.13 (d, J = 4.9 Hz, 1H), 9.20 (d, J = 4.9 Hz, 1H); ^{13}C NMR ($CDCl_3$, 75 MHz, ppm) δ 108.24, 121.71, 121.84, 123.76, 126.92, 127.17, 127.21, 128.12, 128.27, 128.44, 128.75, 129.06, 129.35, 129.89, 130.04, 130.23, 130.61, 134.54, 134.69, 134.93, 135.12, 136.20, 136.24, 138.13, 138.25, 139.96, 140.44, 140.82, 140.94, 142.37, 142.41, 142.47, 142.99, 148.99, 159.09, 159.27; MS (MALDI) m/z 659.82 ([M − Br]$^+$); UV−vis−NIR (CH_2Cl_2, λ_{max}/nm (log ε)) 721 (4.24), 654 (4.07), 484 (5.20), 376 (4.67). Anal. Calcd for **9a**·1.25CH_2Cl_2 ($C_{45.25}H_{30.5}BrCl_{2.5}N_5O_2$): C, 64.33; H, 3.64; N, 8.29. Found: C, 64.41; H, 3.71; N, 8.21.

3-Bromo-21-nitro N-confused 5,10,15,20-tetrakis(4-methylphenyl)porphyrin (9b): Starting from **8b** (131.4 mg, 0.18 mmol) in 40 mL of CH_2Cl_2, **9b** was obtained in 75% yield (107 mg, 0.13 mmol). ^{1}H NMR ($CDCl_3$, 300 MHz, ppm) δ −2.03 (br, 2H), 2.68 (s, 3H), 2.69 (s, 6H), 2.72 (s, 3H), 7.54−7.61 (m, 4H), 7.68−7.72 (m, 4H), 7.89 (d, J = 7.3 Hz, 1H), 7.98 (d, J = 7.3 Hz, 2H), 8.12 (d, J = 6.4 Hz, 1H), 8.32 (d, J = 4.4 Hz, 2H), 8.34 (d, J = 4.4 Hz, 2H), 8.48 (s, 2H), 8.65 (d, J = 4.9 Hz, 2H), 9.07 (d, J = 4.9 Hz, 1H), 9.13 (d, J = 4.9 Hz, 1H); ^{13}C NMR ($CDCl_3$, 75 MHz, ppm) δ 21.48, 21.59, 21.66, 108.44, 121.59, 121.79, 123.77, 127.61, 127.88, 127.93, 128.21, 128.60, 129.04, 129.29, 129.91, 129.97, 130.13, 130.14, 130.40, 134.54, 134.68, 135.05, 135.27, 135.98, 137.54, 137.99, 138.01, 138.05, 138.09, 138.14, 138.28, 139.27, 139.68, 142.38, 142.51, 143.04, 149.30, 159.06, 159.19; MS (MALDI) m/z 715.40 ([M − Br]$^+$); HRMS (ESI$^+$) found m/z 794.21447, calcd for $C_{48}H_{37}BrN_5O_2$ (MH$^+$) m/z 794.21306; UV−vis−NIR (CH_2Cl_2, λ_{max}/nm (log ε)) 730 (4.19), 665 (3.97), 487 (5.07), 383 (4.55).

3-Bromo-21-nitro N-confused 5,10,15,20-tetrakis(4-*tert*-butylphenyl)porphyrin (9c): Starting from **8c** (107 mg, 0.121 mmol) in 20 mL of CH_2Cl_2, **9c** was obtained in 61% yield (71 mg, 0.074 mmol). ^{1}H NMR ($CDCl_3$, 300 MHz, ppm) δ −2.90 (br, 2H), 1.58 (s, 9H), 1.60 (s, 18H), 1.61 (s, 9H), 7.74−7.82 (m, 4H), 7.90−7.94 (m, 5H), 8.03−8.08 (m, 2H), 8.20−8.23 (m, 1H), 8.37 (d, J = 8.5 Hz, 2H), 8.41 (d, J = 8.5 Hz, 2H), 8.48 (s, 2H), 8.67−8.69 (m, 2H), 9.11 (d, J = 4.9 Hz, 1H), 9.20 (d, J = 4.9 Hz, 1H); ^{13}C NMR ($CDCl_3$, 75 MHz, ppm) δ 31.54, 31.62, 34.92, 35.00, 35.05, 107.88, 121.51, 121.84, 123.20, 123.80, 124.09, 124.16, 125.37, 125.54, 128.30, 128.72, 129.80, 130.05, 130.08, 130.13, 130.46, 134.47, 134.60, 135.02, 135.31, 136.07, 136.14, 137.28, 137.90, 137.96, 138.04, 138.10, 138.25, 142.35, 142.48, 142.61, 143.14, 148.86, 151.11, 151.13, 152.11, 152.92, 159.27, 159.29; MS (MALDI) m/z 882.39 ([M − Br]$^+$); HRMS (ESI$^+$) found m/z 962.39849, calcd for $C_{60}H_{61}BrN_5O_2$ (MH$^+$) m/z 962.40086; UV−vis−NIR (CH_2Cl_2, λ_{max}/nm (log ε)) 731 (4.27), 667 (4.05), 488 (5.14), 384 (4.62).

3-Bromo-21-nitro N-confused 5,10,15,20-tetrakis(4-methoxyphenyl)porphyrin (9d): Starting from **8d** (49.0 mg, 0.060 mmol) in 10 mL of CH_2Cl_2, **9d** was obtained in 79% yield (40.4 mg, 0.047 mmol). ^{1}H NMR ($CDCl_3$, 300 MHz, ppm) δ −2.89 (br, 2H), 4.09 (s, 9H), 4.12 (s, 3H), 7.26−7.35 (m, 4H), 7.43 (d, J = 4.6 Hz, 2H), 7.46 (d, J = 4.6 Hz, 2H), 7.88−7.91 (m, 1H), 8.00−8.02 (m, 2H), 8.15−8.18 (m, 1H), 8.36−8.42 (m, 6H), 8.62 (d, J = 5.1 Hz, 1H), 8.63 (d, J = 4.9 Hz, 1H), 9.05 (d, J = 5.1 Hz, 1H), 9.12 (d, J = 4.9 Hz, 1H); ^{13}C NMR ($CDCl_3$, 75 MHz, ppm) δ 55.58, 55.64, 55.68, 108.99, 112.56, 112.58, 114.02, 114.22, 121.01, 121.33, 123.81, 128.00, 128.50, 129.32, 129.73, 129.77, 130.22, 130.60, 133.43, 133.49, 133.53, 134.16, 135.70, 135.76, 135.82, 136.41, 136.70, 139.41, 139.76, 142.54, 142.65, 142.69, 143.18, 149.69, 159.19, 159.20, 159.71, 159.75, 160.97, 161.35; MS (MALDI) m/z 891.05 ([M − Br]$^+$); UV−vis−NIR (CH_2Cl_2, λ_{max}/nm (log ε)) 742 (3.89), 681 (3.71), 493 (4.72), 397 (4.13). Anal. Calcd for **8d**·0.7CH_2Cl_2 ($C_{48.7}H_{37.4}BrCl_{1.4}N_5O_6$): C, 63.70; H, 4.11; N, 7.63. Found: C, 63.83; H, 4.11; N, 7.65.

3-Bromo-21-nitro N-confused 5,10,15,20-tetrakis(3,4,5-trimethoxyphenyl)porphyrin (9e): Starting from **8e** (30 mg, 0.038 mmol) in 10 mL of CH_2Cl_2, **9e** was obtained in 74% yield (24.2 mg, 0.028 mmol). ^{1}H NMR ($CDCl_3$, 300 MHz, ppm) δ −2.96 (br, 2H), 3.92 (s, 3H), 3.96 (s, 3H), 3.99 (s, 3H), 4.06 (s, 3H), 4.13 (s, 6H), 4.15 (s, 6H), 4.16 (s, 9H), 4.20 (s, 3H), 7.21(s, 1H), 7.35 (s, 2H), 7.51 (s, 1H), 7.66 (s, 4H), 8.57 (d, J = 5.2 Hz, 1H), 8.59 (d, J = 5.2 Hz, 1H), 8.74 (d, J = 5.2 Hz, 1H), 8.77 (d, J = 4.9 Hz, 1H), 9.15 (d, J = 5.2 Hz, 1H), 9.26 (d, J = 4.9 Hz, 1H); ^{13}C NMR ($CDCl_3$, 75 MHz, ppm) δ 56.32, 56.36, 56.42, 56.54, 56.64, 56.84, 61.15, 61.27, 61.59, 112.54, 112.64, 112.89, 113.02, 116.08, 116.19, 121.32, 121.39, 124.43, 128.33, 128.54, 129.90, 130.12, 130 23, 130.44, 130.55, 135.97, 136.15, 136.18, 136.24, 136.31, 136.34, 138.13, 138.16, 139.66, 140.52, 142.36, 142.41, 143.11, 149.51, 151.51, 151.61, 151.63, 152.72, 153.26, 159.10, 159.43; HRMS (ESI$^+$) found m/z 1098.27481, calcd for $C_{56}H_{53}BrN_5O_{14}$ (MH$^+$) m/z 1098.27724; UV−vis (CH_2Cl_2, λ_{max}/nm (log ε)) 730 (4.30), 667 (4.11), 494 (5.23), 383 (4.58).

General Procedures for Ring-Fusion of 3-Br-21-NO_2-NCP (9). A pyridine solution (20 mL) of **9** was heated at 80 °C. After cooling, the solvent was removed under reduced pressure and the residue was purified by a silica gel column chromatography eluted with CH_2Cl_2. The red fraction collected was concentrated until dryness to give **1**.

21-Nitro N-fused 5,10,15,20-tetraphenylporphyrin (1a): Starting from **9a** (77 mg, 0.104 mmol), **1a** was obtained in 82% yield (56 mg, 0.085 mmol); reaction time 3 h. ^{1}H NMR ($CDCl_3$, 300 MHz, ppm) δ 5.56 (br s, 1H), 7.66−7.68 (m, 1H), 7.72−7.83 (m, 11H), 7.95 (d, J = 4.9 Hz, 1H), 8.06 (d, J = 6.8 Hz, 1H), 8.12−8.18 (m, 4H), 8.24 (d, J = 7.8 Hz, 2H), 8.35 (d, J = 4.9 Hz, 1H), 8.36 (d, J = 4.9 Hz, 1H), 8.43 (d, J = 4.4 Hz, 1H), 8.97 (d, J = 4.9 Hz, 1H), 9.18 (d, J = 4.9 Hz, 1H); ^{13}C NMR ($CDCl_3$, 75 MHz, ppm) δ 117.49, 120.52, 122.25, 123.34, 126.88, 127.39, 127.96, 128.21, 128.30, 128.38, 128.57, 128.61, 128.96, 129.01, 130.28, 131.33, 131.92, 133.04, 133.23, 133.34, 133.54, 135.00, 136.60, 137.96, 138.60, 138.82, 141.52, 142.27, 144.51, 145.88, 147.90, 149.42, 155.54, 156.09; MS (MALDI) m/z 657.32 ([M]$^+$); UV−vis−NIR (CH_2Cl_2, λ_{max}/nm (log ε)) 837 (3.40), 651 (3.90), 548 (4.65), 526 (4.74), 374 (4.49); R_f 0.75 (CH_2Cl_2/MeOH 98/2). Anal. Calcd for **1a**·0.1CH_2Cl_2 ($C_{44.1}H_{27.2}Cl_{0.2}N_5O_2$): C, 79.51; H, 4.12; N, 10.51. Found: C, 79.45; H, 4.15; N, 10.48.

21-Nitro N-fused 5,10,15,20-tetrakis(4-methylphenyl)porphyrin (1b): Starting from **9b** (107 mg, 0.134 mmol), **1b** was obtained in 67% yield (64 mg, 0.090 mmol); reaction time 2 h. ^{1}H NMR ($CDCl_3$, 300 MHz, ppm) δ 2.59 (s, 3H), 2.64 (s, 6H), 2.70 (s, 3H), 5.54 (br s, 1H), 7.51 (d, J = 7.8 Hz, 2H), 7.57−7.59 (m, 6H), 7.93 (d, J = 7.8 Hz, 2H), 7.96 (d, J = 4.4 Hz, 1H), 8.02 (d, J = 7.8 Hz, 2H), 8.08 (d, J = 7.8 Hz, 2H), 8.13 (d, J = 7.8 Hz, 2H), 8.33 (d, J = 4.4 Hz, 1H), 8.34 (d, J = 4.4 Hz, 1H), 8.40 (d, J = 3.9 Hz, 1H), 8.95 (d, J = 5.2 Hz, 1H), 9.12 (d, J = 5.2 Hz, 1H); ^{13}C NMR ($CDCl_3$, 75 MHz, ppm) δ 21.44, 21.55, 21.58, 21.67, 117.48, 120.33, 121.91, 123.10, 127.39, 127.47, 128.77, 128.95, 129.01, 129.15, 129.38, 130.34, 130.54, 131.30, 131.91, 132.92, 132.96, 133.23, 133.41, 135.13, 135.88, 136.21, 136.34, 137.75, 137.87, 138.40, 138.66, 138.92, 141.94, 142.31, 143.05, 144.94, 147.86, 149.27, 155.16, 155.71; MS (MALDI) m/z 713.45 ([M]$^+$); UV−vis−NIR (CH_2Cl_2, λ_{max}/nm (log ε)) 839 (3.58), 656 (3.98), 554 (4.73), 527 (4.85), 384 (4.57); R_f 0.67 (CH_2Cl_2/MeOH 98/2).

Anal. Calcd for **1b**·1.15CH_2Cl_2 ($C_{49.15}H_{37.3}Cl_{2.3}N_5O_2$): C, 72.75; H, 4.63; N, 8.63. Found: C, 72.63; H, 4.69; N, 8.62.

21-Nitro N-fused 5,10,15,20-tetrakis(4-*tert*-butylphenyl)porphyrin (1c): Starting from **9c** (71 mg, 0.074 mmol), **1c** was obtained in 60% yield (39 mg, 0.044 mmol); reaction time 2 h. ^{1}H NMR ($CDCl_3$, 300 MHz, ppm) δ 1.50 (s, 9H), 1.55 (s, 18H), 1.61 (s, 9H), 5.57 (br s, 1H), 7.72 (d, J = 7.9 Hz, 2H), 7.75−7.81 (m, 6H), 7.92 (d, J = 4.9 Hz, 1H), 7.98 (d, J = 8.5 Hz, 2H), 8.09 (d, J = 7.9 Hz, 2H), 8.14 (d, J = 7.9 Hz, 2H), 8.18 (d, J = 8.5 Hz, 2H), 8.37 (d, J = 4.3 Hz, 2H), 8.44 (d, J = 4.3 Hz, 1H), 8.96 (d, J = 5.2 Hz, 1H), 9.16 (d, J = 5.2 Hz, 1H); ^{13}C NMR ($CDCl_3$, 75 MHz, ppm) δ 31.44, 31.51, 31.67, 34.89, 34.94, 34.98, 117.28, 120.40, 121.97, 123.13, 123.66, 125.03, 125.34, 125.63, 127.50, 129.00, 129.05, 130.41, 130.53, 131.27, 131.83, 132.79, 132.83, 133.33, 133.46, 135.15, 135.86, 136.08, 136.25, 137.76, 141.99, 142.30, 143.00, 144.90, 147.86, 149.12, 151.13, 151.35, 151.71, 151.99, 155.15, 155.73; MS (MALDI) m/z =882.07 ([M]$^+$); UV−vis−NIR (CH_2Cl_2, λ_{max}/nm (log ε)) 845 (3.61), 658 (4.01), 554 (4.86), 527 (4.88), 384 (4.61); R_f 0.78 (CH_2Cl_2/MeOH 98/2). Anal. Calcd for **1c**·0.1CH_2Cl_2 ($C_{60.1}H_{59.2}Cl_{0.2}N_5O_2$): C, 81.05; H, 6.70; N, 7.86. Found: C, 81.20; H, 6.73; N, 7.82.

21-Nitro N-fused 5,10,15,20-tetrakis(4-methoxyphenyl)porphyrin (1d): Starting from **9d** (40.4 mg, 0.047 mmol), **1d** was obtained in 73% yield (26.7 mg, 0.034 mmol); reaction time 3 h. ^{1}H NMR ($CDCl_3$, 300 MHz, ppm) δ 4.01 (s, 3H), 4.04 (s, 3H), 4.05 (s, 3H), 4.10 (s, 3H), 7.22−7.33 (m, 8H), 7.94 (d, J = 8.3 Hz, 2H), 7.97 (d, J = 4.9 Hz, 1H), 8.07 (d, J = 8.3 Hz, 2H), 8.14 (d, J = 8.3 Hz, 2H), 8.18 (d, J = 8.8 Hz, 2H), 8.29 (d, J = 4.9 Hz, 1H), 8.34 (d, J = 4.4 Hz, 1H), 8.36 (d, J = 4.4 Hz, 1H), 8.91 (d, J = 4.9 Hz, 1H), 9.09 (d, J = 4.9 Hz, 1H); ^{13}C NMR ($CDCl_3$, 75 MHz, ppm) δ 55.48, 55.53, 55.61, 112.20, 113.69, 114.00, 114.30, 117.36, 120.30, 121.58, 126.02, 127.47, 128.89, 130.16, 131.41, 131.45, 132.01, 132.91, 133.39, 133.41, 134.11, 134.30, 135.96, 136.55, 137.46, 138.41, 142.47, 142.80, 145.83, 147.88, 149.09, 159.47, 160.13, 160.39, 160.56; MS (MALDI) m/z 777.35 ([M]$^+$); UV−vis−NIR (CH_2Cl_2, λ_{max}/nm (log ε)) 850 (3.79), 703 (4.16), 664 (4.18), 561 (4.79), 529 (4.99), 404 (4.63), 339 (4.59); R_f 0.37 (CH_2Cl_2/MeOH 98/2). Anal. Calcd for **1d**·0.3CH_2Cl_2 ($C_{48.3}H_{35.6}Cl_{0.6}N_5O_6$): C, 72.22; H, 4.47; N, 8.72. Found: C, 72.21; H, 4.50; N, 8.66.

21-Nitro N-fused 5,10,15,20-tetrakis(3,4,5-trimethoxyphenyl)porphyrin (1e): Starting from **9e** (24 mg, 0.022 mmol), **1e** was obtained in 72% yield (16 mg, 0.016 mmol); reaction time 3 h. ^{1}H NMR ($CDCl_3$, 300 MHz, ppm) δ 3.93 (s, 6H), 4.01 (s, 6H), 4.03 (s, 6H), 4.08 (s, 3H), 4.10 (s, 6H), 4.12 (s, 3H), 4.14 (s, 3H), 4.17 (s, 3H), 5.83 (br s, 1H), 7.35 (d, J = 2.9 Hz, 4H), 7.44 (d, J = 4.9 Hz, 4H), 8.07 (d, J = 4.9 Hz, 1H), 8.39 (d, J = 4.4 Hz, 1H), 8.43 (d, J = 4.4 Hz, 1H), 8.48 (d, J = 4.9 Hz, 1H), 9.09 (d, J = 4.9 Hz, 1H), 9.22 (d, J = 4.9 Hz, 1H); ^{13}C NMR ($CDCl_3$, 75 MHz, ppm) δ 56.36, 56.40, 56.49, 56.51, 61.21, 61.25, 61.37, 61.40, 109.85, 109.92, 111.52, 112.88, 116.86, 120.71, 121.39, 122.59, 127.15, 128.57, 128.84, 129.18, 130.22, 131.30, 133.33, 133.41, 133.94, 134.09, 136.49, 137.98, 138.84, 138.89, 139.37, 141.27, 141.64, 142.15, 147.54, 148.87, 151.52, 152.65, 153.34, 153.61, 155.09, 155.73; MS (MALDI) m/z 778.45 ([M]$^+$), 733.45 ([M − NO_2]$^+$); UV−vis−NIR (CH_2Cl_2, λ_{max}/nm (log ε)) 854 (3.65), 663 (4.06), 561 (4.75), 532 (4.91), 342 (4.59); R_f 0.25 (CH_2Cl_2/MeOH 98/2). Anal. Calcd for **1e**·0.25CH_2Cl_2 ($C_{56.25}H_{51.5}Cl_{0.5}N_5O_{14}$): C, 65.01; H, 4.99; N, 6.74. Found: C, 65.06; H, 4.96; N, 6.63.

21-Nitro N-fused 5,10,15,20-tetrakis(4-trifluoromethylphenyl)porphyrin (1f): To a toluene solution (15 mL) of **3f** (22 mg, 0.023 mmol) were added $AgNO_2$ (3.5 mg, 0.023 mmol) and CH_3CN (2 mL). The resulting mixture was refluxed for 2 h. After cooling, solvent was removed under reduced pressure. The residue was purified by silica gel column chromatography (eluent: dichloromethane/hexane 50/50). The first red fraction collected was concentrated to dryness to give **1f** in 44% yield (9.5 mg, 0.010 mmol). ^{1}H NMR ($CDCl_3$, 300 MHz, ppm) δ 5.42 (br s, 1H), 7.93 (d, J = 4.3 Hz, 1H), 8.03−8.08 (m, 8H), 8.20−8.26 (m, 6H), 8.33−8.36 (m, 3H), 8.41 (m, 2H), 8.98 (d, J = 4.9 Hz, 1H), 9.24 (d, J = 4.9 Hz, 1H); MS (MALDI) m/z 929.40 ([M]$^+$); UV−vis−NIR (CH_2Cl_2, λ_{max}/nm (log ε)) 833 (3.48), 688 (3.89), 529 (4.90), 368 (4.66); R_f 0.73 (CH_2Cl_2/MeOH 99/1). Anal. Calcd for **1f** ($C_{48}H_{23}F_{12}N_5O_2$): C, 62.01; H, 2.49; N, 7.53. Found: C, 61.98; H, 2.40; N, 7.48. It was difficult to obtain a reliable ^{13}C NMR spectrum because of low solubility.

21-Nitro N-fused 5,10,15,20-tetrakis(2,4,6-trimethylphenyl)porphyrin (1g): To a toluene solution (15 mL) of **3g** (20 mg, 0.023 mmol) were added $AgNO_2$ (3.8 mg, 0.025 mmol) and CH_3CN (2 mL). The resulting mixture was refluxed for 2 h. After cooling, the solvent was removed under reduced pressure. The residue was purified by silica gel column chromatography (eluent: dichloromethane/hexane 50/50). The first red fraction collected was concentrated to dryness to give **1g** in 84% yield (16 mg, 0.019 mmol). ^{1}H NMR ($CDCl_3$, 300 MHz, ppm) δ 1.14 (s, 6H), 1.22 (s, 12H), 1.27 (s, 6H), 1.75 (s, 3H), 1.79 (s, 6H), 1.85 (s, 3H), 5.94 (br s, 1H), 7.18−7.20 (m, 6H), 7.26 (2H, overlapped with a peak due to $CHCl_3$), 7.90 (d, J=4.6 Hz, 1H), 8.10 (d, J = 4.6 Hz, 1H), 8.11 (s, 2H), 8.82 (d, J=4.9 Hz, 1H), 8.98 (d, J =4.9 Hz, 1H); ^{13}C NMR ($CDCl_3$, 75 MHz, ppm) δ 21.25, 21.34, 21.37, 21.41, 21.44, 21.48, 21.52, 21.54, 21.75, 21.80, 116.26, 121.94, 125.54, 126.24, 127.79, 127.93, 127.99, 128.07, 128.14, 128.20, 128.35, 128.76, 130.02, 130.65, 132.01, 132.41, 133.99, 134.45, 135.40, 137.54, 137.67, 138.05, 138.12, 138.36, 138.54, 138.78, 139.30, 141.85, 142.32, 143.24, 148.31, 150.95, 156.38, 156.87; MS (MALDI) m/z 825.39 ([M]$^+$); HRMS (ESI$^+$) found m/z 826.41250, calcd for $C_{56}H_{52}N_5O_2$ (MH$^+$) m/z 826.41210; UV−vis−NIR (CH_2Cl_2, λ_{max}/nm) 825 (3.15), 683 (3.56), 528 (4.69), 350 (4.33); R_f 0.81 (CH_2Cl_2/MeOH 98/2).

21-(4-Nitrophenylethynyl) N-fused 5,10,15,20-tetraphenylporphyrin (5a): A solution of **3a** (50 mg, 0.082 mmol, 1 equiv) in THF (10 mL) was treated with 1-ethynyl-4-nitrobenzene (60 mg, 0.42 mmol, 5 equiv) in the presence of $Pd(PPh_3)_4$ (25 mg, 25 mol %) and *n*-tetrabutylammonium acetate (32.7 mg, 0.108 mmol, 1.3 equiv) for 24 h at ambient temperature under argon atmosphere. After removing the solvent under reduced pressure, the residue was separated by a silica gel column chromatography eluted with CH_2Cl_2. The first purple fraction collected was concentrated to dryness to give **5a** in 16% yield (10.1 mg, 0.013 mmol). ^{1}H NMR ($CDCl_3$, 300 MHz, ppm) δ 7.25−7.28 (m, 2H), 7.49 (br s, 1H), 7.60−7.81 (m, 13H), 8.00−8.02 (m, 2H), 8.05−8.08 (m, 3H), 8.12−8.13 (m, 2H), 8.19−8.22 (m, 2H), 8.25−8.28 (m, 2H), 8.71 (d, J = 5.2 Hz, 1H), 8.79−8.82 (m, 2H), 9.11 (d, J = 5.2 Hz, 1H); ^{13}C NMR ($CDCl_3$, 75 MHz, ppm) δ 94.36, 101.39, 101.56, 116.32, 119.91, 120.87, 123.45, 125.54, 126.12, 126.97, 127.78, 127.82, 127.87, 128.24, 128.32, 129.05, 129.29, 130.06, 130.91, 131.25, 131.33, 131.36, 131.68, 133.01, 133.32, 133.35, 133.65, 134.34, 134.43, 135.38, 137.19, 137.37, 138.83, 139.79, 142.10, 145.99, 146.07, 146.64, 150.70, 151.01, 154.72, 157.09; MS (MALDI) m/z 757.08 ([M]$^+$); UV−vis−NIR (CH_2Cl_2, λ_{max}/nm (log ε)) 973 (3.52), 879 (3.52), 724 (4.29), 671 (4.28), 580 (4.94), 533 (4.69), 402 (4.63), 347 (4.70); R_f 0.44 (CH_2Cl_2/MeOH 98/2). Anal. Calcd for **5a**·0.3CH_2Cl_2 ($C_{52.3}H_{31.6}Cl_{0.6}N_5O_2$): C, 80.19; H, 4.07; N, 8.94. Found: C, 80.34; H, 4.08; N, 8.97.

21-Bromo N-fused 5,10,15,20-tetrakis(4-trifluoromethylphenyl)porphyrin (3f): To a solution of **7f** (200 mg, 0.23 mmol, 1.0 equiv) in CH_2Cl_2 was added NBS (86 mg, 0.48 mmol, 2.1 equiv), then the reaction mixture was stirred for 5 min at ambient temperature. Without removing the solvent, the crude reaction mixture was passed through a silica gel chromatography column eluted with CH_2Cl_2 to purify. The second green fraction collected afforded **10f**. A pyridine solution of **10f** was stirred for 12 h at ambient temperature. After evaporation, the residue was purified by a silica gel column chromatography. The first red fraction collected was concentrated to dryness to give **3f** in 46% yield (102 mg, 0.11 mmol). ^{1}H NMR ($CDCl_3$, 300 MHz, ppm) δ 7.47 (d, J = 4.4 Hz, 1H), 7.91 (d, J = 4.4 Hz, 1H), 7.96−8.03 (m, 10H), 8.08−8.18

(m, 6H), 8.54 (d, J = 5.1 Hz, 1H), 8.57 (br, 1H), 8.63−8.65 (m, 2H), 9.01 (d, J = 5.1 Hz, 1H); ^{13}C NMR ($CDCl_3$, 75 MHz, ppm) δ 95.96, 113.35, 118.60, 120.30, 122.49, 124.21, 124.26, 124.68, 124.73, 124.77, 124.82, 124.86, 124.94, 125.70, 126.01, 126.05, 126.10, 128.50, 128.81, 129.64, 129.64, 130.60, 130.20, 130.42, 130.61, 130.85, 131.14, 131.57, 131.69, 132.52, 132.82, 133.07, 133.19, 133.61, 134.10, 135.25, 136.74, 137.35, 138.89, 139.88, 141.30, 142.06, 145.43, 146.78, 149.35, 150.31, 154.54, 157.70; MS (MALDI) m/z 962.30 ([M]$^+$); HRMS (ESI$^+$) found m/z 963.10185, calcd for $C_{48}H_{24}BrF_{12}N_4$ (MH$^+$) m/z 963.09927; UV−vis−NIR (CH_2Cl_2, λ_{max}/nm (log ε)) 953 (3.44), 865 (3.42), 705 (3.62), 650 (3.82), 545 (4.71), 503 (4.73), 367 (4.70).

21-Bromo N-fused 5,10,15,20-tetrakis(2,4,6-trimethylphenyl)-porphyrin (3g): To a solution of **7g** (40 mg, 0.051 mmol, 1.0 equiv) in CH_2Cl_2 was added NBS (17.8 mg, 0.11 mmol, 2.1 equiv), then the reaction mixture was stirred for 5 min at ambient temperature. Without removing the solvent, the crude reaction mixture was passed through a silica gel chromatography column eluted with CH_2Cl_2 to purify. The second green fraction collected afforded **10g**. A pyridine solution of **10g** was stirred for 10 h at 60 °C. After evaporation, the residue was purified by a silica gel column chromatography. The first red fraction collected was concentrated to dryness to give **3g** in 35% yield (17 mg, 0.018 mmol). ^{1}H NMR ($CDCl_3$, 300 MHz, ppm) δ 1.99 (s, 6H), 2.03 (s, 6H), 2.05 (s, 6H), 2.07 (s, 6H), 2.49 (s, 3H), 2.50 (s, 3H), 2.52 (s, 3H), 2.56 (s, 3H), 7.13−7.19 (m, 8H), 7.44 (d, J = 4.9 Hz, 1H), 7.65 (d, J = 4.3 Hz, 1H), 7.73 (d, J = 4.3 Hz, 1H), 7.74 (d, J = 4.9 Hz, 1H), 8.50−8.53 (m, 2H), 9.11 (br, 1H); ^{13}C NMR ($CDCl_3$, 75 MHz, ppm) δ 21.08, 21.18, 21.32, 21.35, 21.39, 21.43, 21.51, 95.14, 112.01, 116.58, 120.34, 123.06, 123.70, 127.85, 127.96, 128.00, 128.32, 128.74, 129.18, 130.34, 131.16, 132.57, 133.13, 133.46, 133.65, 134.86, 135.10, 137.45, 137.66, 137.73, 137.98, 138.15, 138.43, 138.49, 138.52, 138.87, 140.01, 141.93, 144.62, 147.43, 150.29, 154.65, 158.77; MS (MALDI) m/z 858.34 ([M]$^+$); HRMS (ESI$^+$) found m/z 859.33410, calcd for $C_{56}H_{52}BrN_4$ (MH$^+$) m/z 859.33753; UV−vis−NIR (CH_2Cl_2 λ_{max}/nm (log ε)) 940 (3.17), 849 (3.18), 688 (3.39), 636 (3.64), 532 (4.51), 496 (4.57), 343 (4.49); R_f 0.47 (CH_2Cl_2/MeOH 99/1).

N-Fused 5,10,15,20-tetrakis(2,4,6-trimetylphenyl)porphyrin (2g): A mixture of **3g** (16.6 mg, 0.019 mmol, 1.0 equiv), Pd(PPh$_3$)$_4$ (6.6 mg, 0.057 mmol, 0.3 equiv), $C_6F_5B(OH)_2$ (40.3 mg, 0.19 mmol, 10 equiv), and K_2CO_3 (26.3 mg, 0.19 mmol) was dissolved in distilled toluene (3 mL), then the solution was degassed by three freeze−pump−thaw cycles. The resulting mixture was refluxed for 24 h under Ar atmosphere. After evaporation of volatiles, the residue was separated by column chromatography on silica gel eluting with CH_2Cl_2/MeOH 98/2 (v/v). The second red fraction collected was concentrated to dryness to afford **2g** (9.3 mg, 0.012 mmol, 63%). ^{1}H NMR ($CDCl_3$, 300 MHz, ppm) δ 2.00 (s, 6H), 2.06 (s, 6H), 2.08 (s, 6H), 2.10 (s, 6H), 2.48 (s, 3H), 2.52 (s, 3H), 2.53 (s, 3H), 2.58 (s, 3H), 7.15−7.21 (m, 8H), 7.53 (d, J = 4.6 Hz, 1H), 7.74 (d, J = 4.2 Hz, 1H), 7.80 (d, J = 4.2 Hz, 1H), 7.82 (d, J = 4.6 Hz, 1H), 8.49 (s, 1H), 8.54 (d, J=4.9 Hz, 1H), 8.59 (d, J = 4.9 Hz, 1H); ^{13}C NMR ($CDCl_3$, 75 MHz, ppm) δ 20.94, 20.96, 21.20, 21.25, 21.30, 21.34, 21.38, 21.56, 21.59, 107.65, 107.94, 112.16, 116.06, 120.00, 120.28, 120.31, 123.09, 123.35, 127.74, 127.86, 128.00, 128.07, 128.14, 128.27, 128.48, 128.61, 130.73, 130.79, 132.01, 132.81, 133.21, 133.88, 135.17, 137.34, 137.60, 137.94, 138.15, 138.46, 138.57, 139.02, 140.08, 142.09, 147.70, 151.44, 152.05, 153.85, 157.60; MS (MALDI) m/z 780.33 ([M]$^+$); HRMS(ESI$^+$) found m/z 781.42877, calcd for $C_{56}H_{52}N_4$ (MH$^+$) m/z 781.42647; UV−vis−NIR (CH_2Cl_2 λ_{max}/nm (log ε)) 911 (3.21), 828 (3.17), 687 (3.44), 633 (3.59), 489 (4.59), 344 (4.50); R_f 0.09 (CH_2Cl_2/MeOH 99/1).

***N*-Methyl N-fused 5,10,15,20-tetraphenylporphyrinium trifluoromethanesulfonate (11aH$^+$·OSO$_2$CF$_3^-$).** To a dichloromethane (8 mL) solution of **2a** (46 mg, 0.075 mmol, 1.0 equiv) was added methyl trifluoromethanesulfonate (20 μL, 0.23 mmol, 3.0 equiv), and the resulting mixture was stirred for 34 h at ambient temperature. The reaction mixture was poured onto a silica gel column, which was eluted with dichloromethane/ethyl acetate 90/10 (v/v). The second red fraction collected was concentrated to dryness to give **11aH$^+$·OSO$_2$CF$_3^-$** in 73% yield (43 mg, 0.055 mmol). ^{1}H NMR ($CDCl_3$, 300 MHz, ppm) δ −0.41 (s, 3H), 5.73 (br s, 1H), 7.16 (d, J = 4.3 Hz, 1H), 7.23 (d, J = 4.3 Hz, 1H), 7.68−7.73 (m, 2H), 7.81−7.97 (m, 12H), 8.12−8.15 (m, 1H), 8.21−8.23 (m, 2H), 8.50 (d, J = 4.9 Hz, 1H), 8.54 (d, J = 6.1 Hz, 2H), 8.73 (d, J = 5.5 Hz, 1H), 8.75 (d, J = 9.1 Hz, 2H), 9.35 (d, J = 5.5 Hz, 1H), 9.79 (s, 1H); ^{13}C NMR ($CDCl_3$, 75 MHz, ppm) δ 34.79, 113.55, 116.01, 118.44, 118.72, 120.63, 120.75, 124.60, 127.98, 128.17, 129.08, 129.19, 129.59, 130.39, 130.47, 130.58, 131.26, 131.40, 131.64, 131.88, 132.34, 132.39, 132.78, 132.95, 133.34, 133.37, 134.92, 136.74, 137.11, 137.29, 139.49, 140.68, 141.01, 142.36, 146.77, 147.50, 152.65, 153.49, 153.95, 157.56; MS (MALDI) m/z 626.97 ([M − CF_3SO_3]$^+$); UV−vis−NIR (CH_2Cl_2, λ_{max}/nm (log ε)) 953 (3.88), 876 (3.97), 703 (3.93), 650 (3.97), 550 (4.57), 488 (4.87), 372 (4.73); R_f 0.06 (CH_2Cl_2/MeOH 98/2). Anal. Calcd for **11aH$^+$·OSO$_2$CF$_3$** ($C_{46}H_{31}F_3N_4O_3S$): C, 71.12; H, 4.02; N, 7.21. Found: C, 70.94; H, 3.93; N, 7.16.

Calculation Details. All density functional theory (DFT)[24] calculations were achieved with a Gaussian03 program package.[25] The basis sets implemented in the program were used. The B3LYP density functional method[26] was used with the 6-31G** basis set for structural optimizations. The initial structures were constructed based on the related X-ray structures.[5a,b,7b] Equilibrium geometries were fully optimized and verified by the frequency calculations, where no imaginary frequency was found. The time-dependent DFT (TD-DFT) calculations were performed for the optimized structures with the 6-311++G** basis set. The top 20 transitions (30 for **2g**) were calculated in each case. The reliability of the calculations for porphyrinoids at the B3LYP/6-31G** level is supported by the previous theoretical works.[27]

Acknowledgment. The present work was supported by the Grant-in-Aid for Scientific Research (19750036 and 21750047) and the Global COE Program "Science for Future Molecular Systems" from the Ministry of Education, Culture, Sports, Science and Technology of Japan. M.T. thanks Takeda Science Foundation for financial support on this work. The work at Yonsei University was supported by the Star Faculty and WCU (World Class University) programs (*R*32-2008-000-10217-0) through the National Research Foundation of Korea funded by the Ministry of Education, Science and Technology (MEST), and the AFSOR/AOARD grant (no. FA2386-09-1-4092).

Supporting Information Available: ^{1}H and ^{13}C NMR spectra of all new compounds, absorption spectra of **1a** and **2a** in various solvents, Cartesian coordinates for the optimized structures, and crystallographic data of **11aH$^+$·OSO$_2$CF$_3$** in CIF format. This material is available free of charge via the Internet at http://pubs.acs.org.

(24) (a) Hohenberg, P.; Kohn, W. *Phys. Rev.* **1964**, *136*, B864. (b) Kohn, W.; Sham, L. *J. Phys. Rev.* **1965**, *140*, A1133.

(25) Frisch, M. J. et al. . *Gaussian 03*, Revision D.01; Gaussian, Inc., Wallingford, CT, 2004.

(26) (a) Becke, A. D. *J. Phys. Chem.* **1993**, *98*, 5648. (b) Lee, C.; Yang, W.; Parr, R. G. *Phys. Rev. B* **1988**, *37*, 785. (c) Vosko, S. H.; Wilk, L.; Nusair, M. *Can. J. Phys.* **1980**, *58*, 1200. (d) Stephens, P. J.; Devlin, F. J.; Chabalowski, C. F.; Frisch, M. J. *J. Phys. Chem.* **1994**, *98*, 11623.

(27) (a) Szterenberg, L.; Latos-Grażyński, L. *J. Porphyrins Phthalocyanines* **2001**, *5*, 474. (b) Furuta, H.; Maeda, H.; Osuka, A. *J. Org. Chem.* **2000**, *65*, 4222. (c) Furuta, H.; Maeda, H.; Osuka, A. *J. Org. Chem.* **2001**, *66*, 8563. (d) Vyas, S.; Hadad, C. M.; Modarelli, D. A. *J. Phys. Chem. A* **2008**, *112*, 6533. (e) Ghosh, A. *Angew. Chem., Int. Ed. Engl.* **1995**, *34*, 1028. (f) Kiran, B.; Nguyen, M. T. *J. Organomet. Chem.* **2002**, *643*−*644*, 265. (g) Toganoh, M.; Furuta, H. *J. Phys. Chem. A* **2009**, *113*, 11953.